Eur. Phys. J. A **9**, 521–536 (2000)

THE EUROPEAN PHYSICAL JOURNAL A

Antikaon production and medium effects in proton-nucleus reactions at subthreshold beam energies

E.Ya. Paryev[a]

Institute for Nuclear Research, Russian Academy of Sciences, Moscow 117312, Russia

Received: 20 July 2000 / Revised version: 10 November 2000
Communicated by W. Weise

Abstract. The inclusive K^--meson production in proton-nucleus collisions in the subthreshold energy regime is analyzed in the framework of an appropriate folding model for incoherent primary proton-nucleon and secondary pion-nucleon production processes, which takes properly into account the struck target nucleon momentum and removal energy distribution (nucleon spectral function), novel elementary cross-sections for proton-nucleon reaction channel close to threshold as well as nuclear mean-field potential effects on the one-step and two-step antikaon creation processes. A detailed comparison of the model calculations of the K^- differential cross-sections for the reactions $p + {}^9Be$ and $p + {}^{63}Cu$ at subthreshold energies with the first experimental data obtained at the ITEP proton synchrotron is given, that displays both the relative role of the primary and secondary production channels at considered incident energies and the contributions to the K^- production coming from the use of the single-particle part as well as high-momentum-energy part of the nucleon spectral function. It is found that the pion-nucleon production channel does not dominate in the subthreshold "hard" antikaon production in $p{}^9Be$-, $p{}^{63}Cu$-collisions and the main contributions to the antikaon yields here come from the direct K^- production mechanism. The influence of the nucleon, kaon and antikaon mean-field potentials on the K^- yield is explored. It is shown that the effect of the nucleon mean-field is of importance in explaining the considered experimental data on "hard" antikaon production, whereas the K^+ and K^- optical potentials play a minor role. The sensitivity of the subthreshold "soft" antikaon production in $p{}^9Be$-, $p{}^{12}C$-reactions to the nucleon, kaon and antikaon mean fields is studied. It is demonstrated that, contrary to the case of "hard" antikaon production, the K^- potential has a very strong effect on the K^- yield, which is greater than that from nucleon effective potential.

PACS. 25.40.-h Nucleon-induced reactions

1 Introduction

Kaon and antikaon properties in dense matter are a subject of considerable current interest in the nuclear physics commynity [1]. The knowledge of these properties is important for understanding both chiral symmetry restoration in dense nuclear medium and neutron star properties. Since the pioneering work of Kaplan and Nelson [2] on the possibility of kaon condensation in nuclear matter, there have been many theoretical studies on the in-medium properties of kaons and antikaons, based on various approaches such as the effective chiral Lagrangian [3–8], the boson exchange model [8–10], the Namby-Jona-Lasinio model [11,12], the quark-meson coupling model [13], the coupled-channel [14,15] and effective KN scattering length [16] approaches. Although these models give quantitatively different predictions for the kaon and antikaon potentials in a nuclear medium, they agree qualitatively in establishing that in nuclear matter the K^+ feels a weak repulsive potential of about 20–30 MeV at normal nuclear matter density ρ_0 ($\rho_0 = 0.17\,\mathrm{fm}^{-3}$), whereas the K^- feels a strong attractive potential which ranges between -140 and -75 MeV at ρ_0. The K^- atomic data also indicate [10, 17,18] that the real part of the antikaon optical potential can be of the order of $\approx -200 \pm 20$ MeV at normal nuclear matter density while being slightly repulsive at very low densities in accordance with the K^-p scattering length. As a result, the deeply bound kaonic nuclei should exist [19]. Moreover, a condensation of antikaons in neutron stars at critical density of about $3\rho_0$ becomes possible, which would then lead to the lowering of the maximum neutron star mass to the value that is in a good agreement with the observed one as well as to the existence of a large number of low mass black holes in galaxy [20]. On the other hand, in the recent chiral approach of Oset and Ramos [21] was shown that as nuclear density ρ_N increases the attraction felt by the K^- is essentially more moderate than that obtained with other theories and the effective K^- mass $m^*_{K^-}$ gains at high densities the level

[a] e-mail: paryev@al20.inr.troitsk.Ru

around the value achieved already at $\rho_N = \rho_0$, namely: $m^*_{K^-}(\rho_N > \rho_0) \approx m^*_{K^-}(\rho_N = \rho_0) = 445\,\mathrm{MeV}$, what makes very unlikely the appearance of the phenomenon of K^- condensation in neutron star matter. The in-medium K^- mass of 445 MeV corresponds to a weaker attractive K^- optical potential of about $-50\,\mathrm{MeV}$ at normal nuclear matter density. Furthermore, coupled-channel calculations for antikaons in matter performed very recently in [22] have demonstrated that the K^- optical potential turns repulsive for finite momenta or finite temperature. The momentum dependence of the K^+ and K^- potentials at finite nuclear density has been investigated in [23, 24] within the dispersion approach. It was obtained, that contrary to [22], the antikaon potential remains attractive even at high momenta. The K^- potential of $\approx -28\,\mathrm{MeV}$ at density ρ_0 and an antikaon momentum of $800\,\mathrm{MeV/c}$ has been extracted in [25] from the data on elastic K^-A scattering within Glauber theory. Therefore, it is very important to have such experimental data which allow one to test the predictions of the above models.

Subthreshold kaon and antikaon production in heavy-ion collisions in which the high densities are accessible is apparently best suited for the studying of their properties in dense matter. The transport model calculations [1, 26–33] have shown that the in-reaction-plane and out-of reaction-plane kaon flow is a sensitive probe of K^+ potential in medium. The dropping K^- mass scenario will lead to a substantial enhancement of the K^- yield in heavy-ion collisions at subthreshold incident energies due to in-medium shifts of the elementary production thresholds to lower energies. Antikaon enhancement in nucleus-nucleus interactions has been recently observed by the KaoS and FRS Collaborations at SIS/GSI [34–38]. This phenomenon has been attributed to the in-medium K^- mass reduction [16,20,39–42]. Thus, analysis of the KaoS data [34,35] within the framework of a relativistic transport model [20, 39–41] has shown that these data are consistent with the predictions of the chiral perturbation theory that the K^+ feels a weak repulsive potential and the K^- feels a strong attractive potential in the nuclear medium (respectively, of about 20 and $-110\,\mathrm{MeV}$ at normal nuclear matter density). This is similar to the findings of Cassing *et al.* [42].

A special question regards the validity of extrapolation of extracted in [20,39–42] an "empirical" kaon and antikaon dispersion relations from densities of $(2\text{–}3)\rho_0$ to the density of ordinary nuclei. This can be clarified from the study of subthreshold K^+ and K^- production in proton-induced reactions. The advantage of these reactions is that a possible kaon and antikaon mass changes (up to 5% and 20% for K^+ and K^-, respectively), although smaller than those in heavy-ion collisions, can be better controlled due to their simpler dynamics compared to the case of nucleus-nucleus interactions. Therefore, the information obtained from the proton-induced reactions will supplement that deduced from heavy-ion collision studies and provide an independent test of theoretical predictions that precursor phenomena of chiral symmetry restoration should be observable already at normal nuclear matter density.

Another very important information that can be extracted from the study of K^+- and K^--meson production in pA-collisions at subthreshold incident energies concerns such intrinsic properties of target nuclei as Fermi motion, high momentum components of the nuclear wave function.

The inclusive K^+ production in proton-nucleus reactions at bombarding energies less than threshold energies in a collision of free nucleons has been extensively studied both experimentally and theoretically in recent years [43–55]. This phenomenon is under studying presently at the accelerators COSY-Jülich [56] and CELSIUS [57] as well as at the ITEP proton synchrotron [58,59]. Up to now, there have been, however, no data on subthreshold K^- production in proton-nucleus collisions. Recently, such experimental data have been obtained at the ITEP proton synchrotron [60]. The main goal of the present work is to analyze these data within the spectral function approach. In the paper we present the analysis of the first experiment [60] on subthreshold K^- production on Be and Cu target nuclei by protons. Some preliminary results of this analysis have been reported in [60]. It should be noted that the investigation of inclusive and exclusive subthreshold K^- production in pA-interactions is planned in the near future at the accelerator COSY-Jülich [56].

The paper is organized as follows. In section 2 we give a review of the spectral function approach employed as well as the parametrizations for the elementary antikaon production cross-sections. In section 3 we present a detailed comparison of our calculations with the data [60] as well as our predictions for the differential cross-sections for "soft" K^- production on ^{9}Be and ^{12}C target nuclei, which might be measured at, for example, the Cooler Synchrotron COSY-Jülich. Finally, the results of this study are summarized in section 4.

2 The model and inputs

2.1 Direct K^- production mechanism

Apart from participation in the elastic scattering an incident proton can produce a K^- directly in the first inelastic pN-collision due to nucleon Fermi motion. Since we are interested in a few GeV region (up to 3 GeV), we have taken into account [61] the following elementary process which has the lowest free production threshold (2.99 GeV for kinematical conditions of the experiment [60] in which the rather "hard" K^--mesons with momentum of $1.28\,\mathrm{GeV/c}$ at the laboratory angle of 10.5° have been detected):

$$\mathrm{p} + \mathrm{N} \longrightarrow \mathrm{N} + \mathrm{N} + \mathrm{K} + \mathrm{K}^-, \qquad (1)$$

where K stands for K^+ or K^0 for the specific isospin channel. In the following calculations, we will include the medium modification of the final hadrons (nucleons, kaon and antikaon) participating in the production process (1) by using their in-medium masses m^*_h determined below. The kaon and antikaon masses in the medium $m^*_{K^\pm}$ can

be obtained from the mean-field approximation to the effective chiral Lagrangian [27,62,63], *i.e.*

$$m^*_{\mathrm{K}^\pm}(\rho_{\mathrm{N}}) \approx m_{\mathrm{K}}\left(1 - \frac{\Sigma_{\mathrm{KN}}}{2f^2 m^2_{\mathrm{K}}}\rho_{\mathrm{S}} \pm \frac{3}{8f^2 m_{\mathrm{K}}}\rho_{\mathrm{N}}\right), \quad (2)$$

where m_{K} is the rest mass of a kaon in free space, $f = 93\,\mathrm{MeV}$ is the pion decay constant, and Σ_{KN} is the KN sigma term which depends on the strangeness content of a nucleon and reflects the explicit chiral symmetry breaking due to the non-zero strange quark mass. It determines the strength of the attractive scalar potential for kaon and antikaon. The scalar and nuclear densities are denoted, respectively, by ρ_{S} and ρ_{N}. Since the exact value of Σ_{KN} and the size of the higher-order corrections leading to different scalar attractions for kaon and antikaon are not very well known, the quantity Σ_{KN} has been treated in [20,39] as a free parameter which was adjusted separately for K^+ and K^- so that to achieve in the framework of the relativistic transport model a good fits to the experimental K^+ and K^- spectra [34,35] in heavy-ion collisions. Using the values of the "empirical kaon and antikaon sigma terms" obtained in [20,39] and taking into account that $\rho_{\mathrm{S}} \approx 0.9\rho_{\mathrm{N}}$ at $\rho_{\mathrm{N}} \leq \rho_0$ [27], we can readily rewrite eq. (2) in the form

$$m^*_{\mathrm{K}^\pm}(\rho_{\mathrm{N}}) = m_{\mathrm{K}} + U_{\mathrm{K}^\pm}(\rho_{\mathrm{N}}), \quad (3)$$

where the $\mathrm{K}^\pm$ optical potentials $U_{\mathrm{K}^\pm}(\rho_N)$ are proportional to the nuclear density ρ_{N}

$$U_{\mathrm{K}^\pm}(\rho_{\mathrm{N}}) = U^0_{\mathrm{K}^\pm}\frac{\rho_{\mathrm{N}}}{\rho_0} \quad (4)$$

and

$$U^0_{\mathrm{K}^+} = 22\,\mathrm{MeV}, \quad U^0_{\mathrm{K}^-} = -126\,\mathrm{MeV}. \quad (5)$$

To explore the sensitivity of the K^- spectra from primary channel (1) in proton-nucleus reactions to the $\mathrm{K}^\pm$ potentials in nuclear matter, we will both ignore these potentials in our calculations and adopt also in them instead of antikaon potential (4), (5) the K^- potential extracted [17] from the analysis of kaonic atom data, viz.

$$U_{\mathrm{K}^-}(\rho_{\mathrm{N}}) = -129\left[-0.15 + 1.7\left(\frac{\rho_{\mathrm{N}}}{\rho_0}\right)^{0.25}\right]\frac{\rho_{\mathrm{N}}}{\rho_0}\,\mathrm{MeV}. \quad (6)$$

It is easily seen that the potential (6) amounts to $-200\,\mathrm{MeV}$ in the nuclear interior. According to the predictions of the quark-meson coupling model by Tsushima *et al.* [13], one has that $m^*_{\mathrm{K}^0} = m^*_{\mathrm{K}^+}$ in symmetric nuclear matter. The effective mass m^*_{N} of secondary nucleons produced in the reaction (1) can be expressed *via* the scalar mean-field potential $U_{\mathrm{N}}(\rho_{\mathrm{N}})$ as follows [53]:

$$m^*_{\mathrm{N}}(\rho_{\mathrm{N}}) = m_{\mathrm{N}} + U_{\mathrm{N}}(\rho_{\mathrm{N}}), \quad (7)$$

where m_{N} is the bare nucleon mass. The potential $U_{\mathrm{N}}(\rho_{\mathrm{N}})$ was assumed to be proportional to the nuclear density [21]:

$$U_{\mathrm{N}}(\rho_{\mathrm{N}}) = U^0_{\mathrm{N}}\frac{\rho_{\mathrm{N}}}{\rho_0} \quad (8)$$

with the depth at nuclear saturation density ρ_0 relevant [53] for the momentum range of outgoing nucleons for the most part of kinematical conditions of the experiment [60] on subthreshold antikaon production

$$U^0_{\mathrm{N}} = -34\,\mathrm{MeV}. \quad (9)$$

To see the sensitivity of antikaon production cross-sections from the one-step process (1) to the effective nucleon potential, we will both neglect this potential in the following calculations and employ in them the potential of the type (8) with depth [21,52]

$$U^0_{\mathrm{N}} = -50\,\mathrm{MeV}. \quad (10)$$

The total energies E'_h of secondary hadrons inside the nuclear medium can be expressed through their effective masses m^*_h defined above and in-medium momenta $\mathbf{p}'_h$ as in the free particle case, namely

$$E'_h = \sqrt{\mathbf{p}'^2_h + m^{*2}_h}. \quad (11)$$

It should be pointed out that the use of the quasiparticle dispersion relation (11) with momentum-independent scalar potentials (4)–(6), entering into the in-medium masses of final $\mathrm{K}^\pm$-mesons, is very well justified for the K^+-meson [23], whereas in the case of K^--meson it is valid only for small momenta. However, for reasons of simplicity as well as in view of the substantial uncertainties of the model K^- optical potential (see, above), we will neglect the explicit momentum dependence of antikaon mean-field potential in the present study.

Now, let us specify the energies and momenta of incoming proton inside the target nucleus as well as of the struck target nucleon participating in the first chance pN-collision (1) . The total energy E'_0 and momentum $\mathbf{p}'_0$ of the incident proton inside the target nucleus are related to those E_0 and $\mathbf{p}_0$ outside the nucleus by the following expressions [53]:

$$E'_0 = E_0 - \frac{\Delta\mathbf{p}^2}{2M_A}, \quad (12)$$

$$\mathbf{p}'_0 = \mathbf{p}_0 - \Delta\mathbf{p}, \quad (13)$$

where

$$\Delta\mathbf{p} = \frac{E_0 V_0}{p_0}\frac{\mathbf{p}_0}{|\mathbf{p}_0|}. \quad (14)$$

Here, M_A is the mass of the initial target nucleus, and V_0 is the nuclear optical potential that a proton impinging on a nucleus at the kinetic energy ϵ_0 of about a few GeV feels in the interior of the nucleus ($V_0 \approx 40\,\mathrm{MeV}$). Further, let E_{t} and $\mathbf{p}_{\mathrm{t}}$ be the total energy and momentum of the struck target nucleon N just before the collision (1). Taking into account the respective recoil and excitation energies of the residual $(A-1)$ system, one has [52,53]

$$E_{\mathrm{t}} = M_A - \sqrt{(-\mathbf{p}_{\mathrm{t}})^2 + (M_A - m_{\mathrm{N}} + E)^2}, \quad (15)$$

where E is the removal energy of the struck target nucleon. After specifying the energies and momenta all particles involved in the K^- production process (1), we can write out the corresponding energy and momentum conservation:

$$E'_0 + E_t = E'_{N_1} + E'_{N_2} + E'_K + E'_{K^-}, \quad (16)$$

$$\mathbf{p}'_0 + \mathbf{p}_t = \mathbf{p}'_{N_1} + \mathbf{p}'_{N_2} + \mathbf{p}'_K + \mathbf{p}'_{K^-}. \quad (17)$$

From (16) and (17) we obtain the squared invariant energy available in the first chance pN-collision:

$$s = (E'_0 + E_t)^2 - \left(\mathbf{p}'_0 + \mathbf{p}_t\right)^2. \quad (18)$$

On the other hand, according to the eqs. (16), (17), one gets

$$s = \left(E'_{N_1} + E'_{N_2} + E'_K + E'_{K^-}\right)^2 - \left(\mathbf{p}'_{N_1} + \mathbf{p}'_{N_2} + \mathbf{p}'_K + \mathbf{p}'_{K^-}\right)^2. \quad (19)$$

Using (11), this leads to the following expression for the in-medium reaction threshold:

$$\sqrt{s^*_{th}} = 2m^*_N + m^*_{K^+} + m^*_{K^-} = \sqrt{s_{th}} + 2U_N + U_{K^+} + U_{K^-}, \quad (20)$$

where $\sqrt{s_{th}} = 2(m_N + m_K)$ is the threshold energy in free space and the effective potentials are given by (4)–(6), (8)–(10). It is clear from (20) that the threshold for antikaon production in the reaction $pN \to NNKK^-$ is lowered when the in-medium masses are used. Thus, for example, the reduction of the K^- threshold in the nuclear interior will be 172 MeV and 204 MeV, respectively, for potentials (5), (9) and (5), (10). This will strongly enhance the K^- production in first chance pN-collisions at subthreshold beam energies.

Finally, neglecting the K^- production *via* resonances in pN-collisions[1] [16] and taking into consideration the antikaon final-state absorption, we can represent the invariant inclusive cross-section for the production on nuclei K^--mesons with the total energy E_{K^-} and momentum $\mathbf{p}_{K^-}$ from the primary proton induced reaction channel (1) as follows (see, also, [52,53]):

$$E_{K^-}\frac{d\sigma^{(prim)}_{pA\to K^-X}(\mathbf{p}_0)}{d\mathbf{p}_{K^-}} = A\int \rho(\mathbf{r})\,d\mathbf{r} \times \exp\left[-\mu(p_0)\int_{-\infty}^{0}\rho(\mathbf{r}+x\Omega_0)\,dx - \mu(p_{K^-}) \times \int_0^{+\infty}\rho(\mathbf{r}+x\Omega_{K^-})\,dx\right] \times \left\langle E'_{K^-}\frac{d\sigma_{pN\to NNKK^-}\left[\mathbf{p}'_0, \mathbf{p}'_{K^-}, \rho(\mathbf{r})\right]}{d\mathbf{p}'_{K^-}}\right\rangle, \quad (21)$$

where

$$\left\langle E'_{K^-}\frac{d\sigma_{pN\to NNKK^-}[\mathbf{p}'_0, \mathbf{p}'_{K^-}, \rho(\mathbf{r})]}{d\mathbf{p}'_{K^-}}\right\rangle = \iint P(\mathbf{p}_t, E)\,d\mathbf{p}_t\,dE \times \left[E'_{K^-}\frac{d\sigma_{pN\to NNKK^-}\left[\sqrt{s}, \mathbf{p}'_{K^-}, \rho(\mathbf{r})\right]}{d\mathbf{p}'_{K^-}}\right]; \quad (22)$$

$$\mu(p_0) = \sigma^{in}_{pp}(p_0)Z + \sigma^{in}_{pn}(p_0)N,$$

$$\mu(p_{K^-}) = \sigma^{tot}_{K^-p}(p_{K^-})Z + \sigma^{tot}_{K^-n}(p_{K^-})N. \quad (23)$$

Here, $E'_{K^-}\,d\sigma_{pN\to NNKK^-}[\sqrt{s}, \mathbf{p}'_{K^-}, \rho(\mathbf{r})]/d\mathbf{p}'_{K^-}$ is the "in-medium" invariant inclusive cross-section for K^- production in reaction (1); $\rho(\mathbf{r})$ and $P(\mathbf{p}_t, E)$ are the density and nucleon spectral function normalized to unity; $\mathbf{p}_t$ and E are the internal momentum and removal energy of the struck target nucleon just before the collision; σ^{in}_{pN} and $\sigma^{tot}_{K^-N}$ are the inelastic and total cross-sections of free pN- and K^-N-interactions; Z and N are the numbers of protons and neutrons in the target nucleus ($A = N + Z$); $\Omega_0 = \mathbf{p}_0/p_0$ ($\mathbf{p}_0$ is the beam momentum), $\Omega_{K^-} = \mathbf{p}_{K^-}/p_{K^-}$; s is the pN center-of-mass energy squared. The expression for s is given above by the formula (18). In eq. (21) it is assumed that the K^--meson production cross-sections in pp- and pn-interactions are the same [29,61,66] as well as any difference between the proton and the neutron spectral functions is disregarded [52,53]. In addition, it is suggested that the way of the produced antikaon out of the nucleus is not disturbed by the K^- optical potential and K^-N elastic rescatterings as well as that $\sigma^{tot}_{K^-N}(p'_{K^-}) \approx \sigma^{tot}_{K^-N}(p_{K^-})$. Such approximations are allowed in calculating the K^- production cross-sections for kinematics of the experiment [60]. As a result, the in-medium antikaon momentum $\mathbf{p}'_{K^-}$ is assumed to be parallel to the vacuum one $\mathbf{p}_{K^-}$ and the relation between them is given by

$$\sqrt{\mathbf{p}'^2_{K^-} + m^{*2}_{K^-}} = \sqrt{\mathbf{p}^2_{K^-} + m^2_K}. \quad (24)$$

In our approach the invariant inclusive cross-section for K^- production in the elementary process (1) has been described by the four-body phase space calculations nor-

[1] It should be pointed out that in the threshold energy region the K^--mesons can be produced in these collisions also by the decay mainly of the ϕ-meson as an intermediate state [64,65]. Thus, the resonant (ϕ-meson) to non-resonant K^- production cross-section ratio in pp-reactions measured recently by the DISTO Collaboration at SATURNE [65] at a beam energy of 2.85 GeV is equal to 0.82. However, in view of the complete lack of another data in the literature for ϕ-meson production in pp-interactions at energies close to the threshold needed for accurate estimation of the resonant contribution to K^- production in pA-reactions, it is naturally to assume, calculating the K^- yields in pA-collisions from primary channel (1), that the antikaons are produced directly in this channel.

malized to the corresponding total cross-section [52]:

$$E'_{\mathrm{K}^-}\frac{\mathrm{d}\sigma_{\mathrm{pN}\to\mathrm{NNKK}^-}\left[\sqrt{s},\mathbf{p}'_{\mathrm{K}^-},\rho(\mathbf{r})\right]}{\mathrm{d}\mathbf{p}'_{\mathrm{K}^-}}= \sigma_{\mathrm{pN}\to\mathrm{NNKK}^-}\left(\sqrt{s},\sqrt{s^*_{\mathrm{th}}}\right)f_4\left(s,\mathbf{p}'_{\mathrm{K}^-}\right), \quad (25)$$

$$f_4\left(s,\mathbf{p}'_{\mathrm{K}^-}\right)=\frac{I_3(s_{\mathrm{NNK}},m^*_{\mathrm{K}^+},m^*_{\mathrm{N}},m^*_{\mathrm{N}})}{\left[2I_4(s,m^*_{\mathrm{K}^+},m^*_{\mathrm{K}^-},m^*_{\mathrm{N}},m^*_{\mathrm{N}})\right]}, \quad (26)$$

$$I_3\left(s,m^*_{\mathrm{K}^+},m^*_{\mathrm{N}},m^*_{\mathrm{N}}\right)= \left(\frac{\pi}{2}\right)^2\int_{4m^{*2}_{\mathrm{N}}}^{\left(\sqrt{s}-m^*_{\mathrm{K}^+}\right)^2}\frac{\lambda(s_{NN},m^{*2}_{\mathrm{N}},m^{*2}_{\mathrm{N}})}{s_{\mathrm{NN}}} \times\frac{\lambda(s,s_{\mathrm{NN}},m^{*2}_{\mathrm{K}^+})}{s}\,\mathrm{d}s_{\mathrm{NN}}, \quad (27)$$

$$I_4\left(s,m^*_{\mathrm{K}^+},m^*_{\mathrm{K}^-},m^*_{\mathrm{N}},m^*_{\mathrm{N}}\right)= \frac{\pi}{2}\int_{4m^{*2}_{\mathrm{N}}}^{\left(\sqrt{s}-m^*_{\mathrm{K}^+}-m^*_{\mathrm{K}^-}\right)^2}\frac{\lambda(s_{\mathrm{NN}},m^{*2}_{\mathrm{N}},m^{*2}_{\mathrm{N}})}{s_{\mathrm{NN}}} \times I_3\left(s,m^*_{\mathrm{K}^-},\sqrt{s_{\mathrm{NN}}},m^*_{\mathrm{K}^+}\right)\mathrm{d}s_{\mathrm{NN}}, \quad (28)$$

$$\lambda(x,y,z)=\sqrt{\left[x-(\sqrt{y}+\sqrt{z})^2\right]\left[x-(\sqrt{y}-\sqrt{z})^2\right]}, \quad (29)$$

$$s_{\mathrm{NNK}}=s+m^{*2}_{\mathrm{K}^-}-2\left(E'_0+E_{\mathrm{t}}\right)E'_{\mathrm{K}^-}+2\left(\mathbf{p}'_0+\mathbf{p}_{\mathrm{t}}\right)\mathbf{p}'_{\mathrm{K}^-}. \quad (30)$$

Here, $\sigma_{\mathrm{pN}\to\mathrm{NNKK}^-}(\sqrt{s},\sqrt{s^*_{\mathrm{th}}})$ is the "in-medium" total cross-section for K^- production in reaction (1). This cross-section is equivalent [28,42,53] to the vacuum cross-section $\sigma_{\mathrm{pN}\to\mathrm{NNKK}^-}(\sqrt{s},\sqrt{s_{\mathrm{th}}})$ in which the free threshold $\sqrt{s_{\mathrm{th}}}$ is replaced by the effective threshold $\sqrt{s^*_{\mathrm{th}}}$ as given by eq. (20). For the free total cross-section $\sigma_{\mathrm{pN}\to\mathrm{NNKK}^-}(\sqrt{s},\sqrt{s_{\mathrm{th}}})$ we have used the parametrization[2] from [66] that has been corrected[3] for the new data point (2.1 nb) for $\mathrm{pp}\to\mathrm{ppK^+K^-}$ reaction from the COSY-11 collaboration at COSY-Jülich [67] taken at 17 MeV excess energy, viz.:

$$\sigma_{\mathrm{pp}\to\mathrm{ppK^+K^-}}(\sqrt{s},\sqrt{s_{\mathrm{th}}})= \begin{cases} 0.372\left(1-\dfrac{s_{\mathrm{th}}}{s}\right)^{2.72}\ [\mathrm{mb}] \\ \qquad \text{for } 0<\sqrt{s}-\sqrt{s_{\mathrm{th}}}\le 0.1\,\mathrm{GeV}\ , \\ F\left(\dfrac{s}{s_{\mathrm{th}}}\right)\ [\mathrm{mb}] \\ \qquad \text{for } \sqrt{s}-\sqrt{s_{\mathrm{th}}}>0.1\,\mathrm{GeV}, \end{cases} \quad (31)$$

[2] It should be mentioned that this parametrization describes the inclusive $\mathrm{pp}\to\mathrm{K^-}X$ cross-section which is assumed to be the same as that for $\mathrm{pp}\to\mathrm{ppK^+K^-}$ at beam energies of interest [61,66].

[3] It is interesting to note that such correction, as showed by our calculations, leads to reduction of the respective antikaon production cross-sections in pA-collisions only by 1–2% at the beam energies of interest.

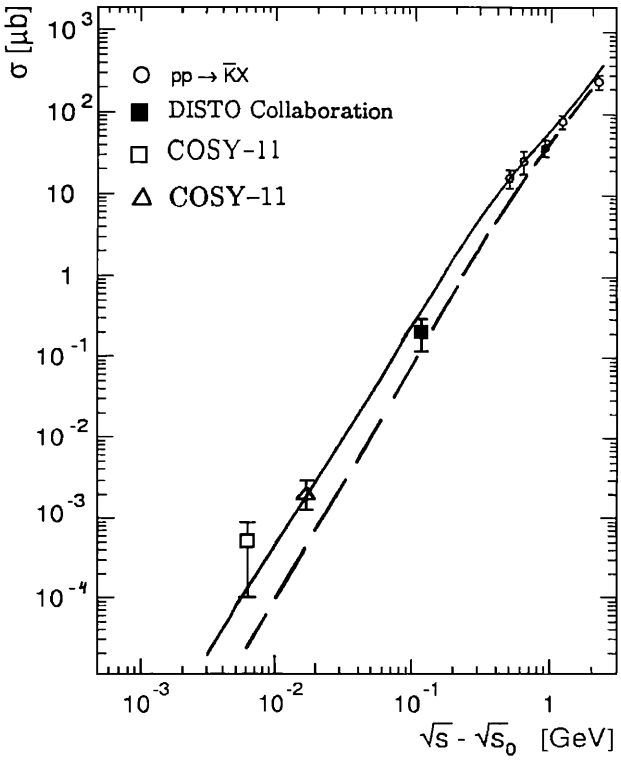

Fig. 1. Total antikaon production cross-section in proton-proton collisions as a function of the available energy above the threshold. For notation see text.

where

$$F(x)=\left(1-\frac{1}{x}\right)^3\left[2.8F_1(x)+7.7F_2(x)\right]+3.9F_3(x), \quad (32)$$

and

$$F_1(x)=(1+1/\sqrt{x})\ln(x)-4(1-1/\sqrt{x}),$$
$$F_2(x)=1-(1/\sqrt{x})(1+\ln(x)/2),$$
$$F_3(x)=\left(\frac{x-1}{x^2}\right)^{3.5}. \quad (33)$$

The comparison of the results of our calculations by (31) (solid line) with the experimental data close to the threshold for $\mathrm{pp}\to\mathrm{ppK^+K^-}$ reaction from the installation COSY-11 (open triangle [67], open square [68]), from the DISTO Collaboration at SATURNE [65] (full square) as well as with the K^- inclusive production cross-sections at higher energies (open circles) [61] is shown in fig. 1. In this figure we also show the predictions from the current parametrization (dashed line) employed in the recent study [23] of the antikaon production in proton-nucleus collisions. It is seen that our parametrization (31) accounts well for the K^- cross-sections measured in the experiments [65,67,68] near the production threshold and is larger than that from [23] at low energies.

For K^- production calculations in the case of ^{9}Be and ^{63}Cu target nuclei reported here we have employed for the

nuclear density $\rho(\mathbf{r})$, respectively, the harmonic oscillator and a two-parameter Fermi density distributions:

$$\rho(\mathbf{r}) = \rho_{\rm N}(\mathbf{r})/A = \frac{(b/\pi)^{3/2}}{A/4}\left\{1+\left[\frac{A-4}{6}\right]br^2\right\}\exp\big(-br^2\big), \quad (34)$$

$$\rho(\mathbf{r}) = \rho_0\left[1+\exp\left(\frac{r-R}{a}\right)\right]^{-1} \quad (35)$$

with $b = 0.329\,\mathrm{fm}^{-2}$ [60] and $R = 4.20\,\mathrm{fm}$, $a = 0.55\,\mathrm{fm}$ [69].

Another very important ingredient for the calculation of the K^- production cross-sections in proton-nucleus reactions in the subthreshold energy regime, *i.e.* the nucleon spectral function[4] $P(\mathbf{p}_{\rm t}, E)$ (which represents the probability to find a nucleon with momentum $\mathbf{p}_{\rm t}$ and removal energy E in the nucleus), for ^{9}Be target nucleus was taken from [52,53], whereas for ^{63}Cu it is assumed to be the same as that for ^{208}Pb [72]. The latter was taken from [73].

Let us now simplify the expression (21) for the invariant differential cross-section for K^- production in pA-collisions from the one-step process. Since we are interested in the spectra of emitted antikaons at forward laboratory angles, *i.e.* when $\Omega_{\mathrm{K}^-} \approx \Omega_0$, we have

$$E_{\mathrm{K}^-}\frac{\mathrm{d}\sigma^{(\rm prim)}_{\mathrm{p}A\to\mathrm{K}^-X}(\mathbf{p}_0)}{\mathrm{d}\mathbf{p}_{\mathrm{K}^-}} = 2\pi A\int_0^{+\infty} r_\perp\,\mathrm{d}r_\perp\int_{-\infty}^{+\infty}\mathrm{d}z\rho\Big(\sqrt{r_\perp^2+z^2}\Big) \times\exp\big[-\mu(p_0,p_{\mathrm{K}^-};r_\perp,z)\big] \times\left\langle E'_{\mathrm{K}^-}\frac{\mathrm{d}\sigma_{\mathrm{pN}\to\mathrm{NNKK}^-}\Big[\mathbf{p}'_0,\mathbf{p}'_{\mathrm{K}^-},\rho\Big(\sqrt{r_\perp^2+z^2}\Big)\Big]}{\mathrm{d}\mathbf{p}'_{\mathrm{K}^-}}\right\rangle, \quad (36)$$

where

$$\mu\big(p_0,p_{\mathrm{K}^-};r_\perp,z\big) = \mu(p_0)t\big(r_\perp,z\big)+\mu(p_{\mathrm{K}^-})t(r_\perp,-z\big) \quad (37)$$

and

$$t(r_\perp,z) = \int_{-\infty}^{z}\rho\Big(\sqrt{r_\perp^2+x^2}\Big)\,\mathrm{d}x. \quad (38)$$

The quantites $\mu(p_0)$ and $\mu(p_{\mathrm{K}^-})$ entering into eq. (37) are defined above by the formula (23). In the case of the harmonic-oscillator density distribution (34) integral (38) has the following simple form:

$$t(r_\perp,z) = \left(\frac{2b}{\pi A}\right)\left\{1+\left[\frac{A-4}{6}\right]br_\perp^2+\left[\frac{A-4}{12}\right] +f(z)-f(-z)\right\}\exp\big(-br_\perp^2\big), \quad (39)$$

$$f(z) = \Theta(z)\left\{\left[1+\left(\frac{A-4}{6}\right)br_\perp^2+\left(\frac{A-4}{12}\right)\right] \times\mathrm{erf}(z\sqrt{b})-\left(\frac{A-4}{6}\right)\frac{z\sqrt{b}}{\sqrt{\pi}}\exp\left(-bz^2\right)\right\},$$

$$\Theta(z) = \frac{(z+|z|)}{2|z|}, \quad \mathrm{erf}(x) = \frac{2}{\sqrt{\pi}}\int_0^x\exp\big(-t^2\big)\,\mathrm{d}t. \quad (40)$$

Taking into account that for K^--mesons with momentum of 1.28 GeV/c the elementary cross-section $\sigma^{\rm tot}_{\mathrm{K}^-\mathrm{N}} \approx 30\,\mathrm{mb}$ [61] as well as that $\sigma^{\rm in}_{\mathrm{pN}} \approx 30\,\mathrm{mb}$ [52] for the beam energy range of interest, we have

$$\mu(p_0) = \mu(p_{\mathrm{K}^-}) = \mu = 30\cdot A\,\mathrm{mb}. \quad (41)$$

Then the expression (37) is reduced to a more simple form:

$$\mu(p_0,p_{\mathrm{K}^-};r_\perp,z) = \mu t(r_\perp), \quad (42)$$

$$t(r_\perp) = t(r_\perp,z)+t(r_\perp,-z) = 2\int_0^{+\infty}\rho\Big(\sqrt{r_\perp^2+x^2}\Big)\,\mathrm{d}x. \quad (43)$$

For the harmonic-oscillator density distribution (34) the quantity $t(r_\perp)$ in view of eqs. (39), (40) has the following simple form:

$$t(r_\perp) = \left(\frac{4b}{\pi A}\right)\left\{1+\left[\frac{A-4}{6}\right]br_\perp^2+\left[\frac{A-4}{12}\right]\right\}\exp\big(-br_\perp^2\big). \quad (44)$$

Let us consider now the two-step K^- production mechanism.

2.2 Two-step K^- production mechanism

Kinematical considerations show that in the bombarding energy range of our interest ($\leq 3.0\,\mathrm{GeV}$) the following two-step production process may not only contribute to the K^- production in pA-interactions but even dominates [23, 70] at subthreshold energies. An incident proton can produce in the first inelastic collision with an intranuclear nucleon also a pion through the elementary reaction

$$\mathrm{p}+\mathrm{N}_1 \longrightarrow \mathrm{N}+\mathrm{N}+\pi. \quad (45)$$

Then the intermediate pion, which is assumed to be on-shell, produces the antikaon on a nucleon of the target nucleus *via* the elementary subprocess with the lowest free production threshold (1.98 GeV for kinematics of the experiment [60]):

$$\pi+\mathrm{N}_2 \longrightarrow \mathrm{N}+\mathrm{K}+\mathrm{K}^-, \quad (46)$$

provided that this subprocess is energetically possible. It is important to note that the elementary processes $\pi\mathrm{N}\to\mathrm{N}\pi\mathrm{K}\mathrm{K}^-$ with one pion in final states, as showed in our calculations with the total cross-sections of these processes taken from [20], play a minor role in subthreshold antikaon production in pA-reactions for kinematics of the experiment [60].

[4] It should be noticed that the full energy-momentum distribution of the struck target nucleons has not been taken into consideration in the previous studies [23,58,70,71] of the subthreshold and near threshold antikaon production in proton-nucleus reactions.

To allow for the influence of the nuclear environment on the secondary K^- production process (46), it is natural to use in calculations of the K^- production cross-section from this process the same in-medium modifications of the masses of final hadrons (kaon, antikaon and nucleon) as those of (3), (7) for hadrons from primary pN-collisions due to the corresponding mean-field potentials $U_{K^\pm}(\rho_N)$ and $U_N(\rho_N)$. For the sake of numerical simplicity, these potentials are assumed here to be density-independent with depths (5) and (9) taken at the nuclear saturation density. Evidently, this enables us to obtain an upper estimation of the respective cross-sections. Moreover, in order to reproduce the high momentum tails of the pion spectra at forward laboratory angles from the reaction (45), which are responsible for the K^- production through the $\pi N \to NKK^-$ channel, it is necessary to take into account in calculating these spectra, as was shown in [53], the modification of the mass of each low-energy nucleon produced together with a high-energy pion by the effective potential (9). But, since we will employ (see, below) in our calculations of the antikaon production from secondary process (46) the pion spectra from proton-nucleus interactions also measured in the experiment [60] instead of the theoretical ones, this modification will be automatically included. Then, taking into account the antikaon final-state absorption as well as using the results given in [52,53], we easily get the following expression for the K^- production cross-section for pA-reactions from the secondary pion-induced reaction channel (46), which includes the medium effects under consideration on the same footing as that employed in calculating the K^- production cross-section (21) from the primary proton-induced reaction channel (1):

$$E_{K^-}\frac{d\sigma^{(sec)}_{pA\to K^-X}(\mathbf{p}_0)}{d\mathbf{p}_{K^-}} = \sum_{\pi=\pi^+,\pi^0,\pi^-}\int_{4\pi}d\Omega_\pi\int_{p_\pi^{abs}}^{p_\pi^{lim}(\vartheta_\pi)}p_\pi^2dp_\pi\frac{d\sigma^{(prim)}_{pA\to\pi X}(\mathbf{p}_0)}{d\mathbf{p}_\pi} \times\frac{I_V\left[A,\sigma^{in}_{pN}(p_0),\sigma^{tot}_{\pi N}(p_\pi),\sigma^{tot}_{K^-N}(p_{K^-}),\vartheta_\pi,\vartheta_{K^-}\right]}{I'_V\left[A,\sigma^{in}_{pN}(p_0),\sigma^{tot}_{\pi N}(p_\pi),\vartheta_\pi\right]} \times\iint P(\mathbf{p}'_t,E')d\mathbf{p}'_t\,dE'\left[E'_{K^-}\frac{d\sigma_{\pi N\to K^-X}(\sqrt{s_1},\mathbf{p}'_{K^-})}{d\mathbf{p}'_{K^-}}\right], \quad (47)$$

where

$$I_V[A,\sigma^{in}_{pN}(p_0),\sigma^{tot}_{\pi N}(p_\pi),\sigma^{tot}_{K^-N}(p_{K^-}),\vartheta_\pi,\vartheta_{K^-}] = A^2\iint d\mathbf{r}\,d\mathbf{r}_1\Theta(x_\parallel)\delta^{(2)}(\mathbf{x}_\perp)\rho(\mathbf{r})\rho(\mathbf{r}_1) \times\exp\left[-\mu(p_0)\int_{-\infty}^{0}\rho(\mathbf{r}_1+x'\Omega_0)\,dx' -\mu(p_\pi)\int_0^{x_\parallel}\rho(\mathbf{r}_1+x'\Omega_\pi)\,dx'\right] \times\exp\left[-\mu(p_{K^-})\int_0^{\infty}\rho(\mathbf{r}+x'\Omega_{K^-})\,dx'\right], \quad (48)$$

$$I'_V\left[A,\sigma^{in}_{pN}(p_0),\sigma^{tot}_{\pi N}(p_\pi),\vartheta_\pi\right] = A\int\rho(\mathbf{r})\,d\mathbf{r} \times\exp\left[-\mu(p_0)\int_{-\infty}^{0}\rho(\mathbf{r}+x\Omega_0)\,dx -\mu(p_\pi)\int_0^{\infty}\rho(\mathbf{r}+x\Omega_\pi)dx\right], \quad (49)$$

$$\mathbf{r}-\mathbf{r}_1 = x_\parallel\Omega_\pi+\mathbf{x}_\perp,\quad \Omega_\pi=\mathbf{p}_\pi/p_\pi,\quad \cos\vartheta_\pi=\Omega_0\Omega_\pi,\quad \cos\vartheta_{K^-}=\Omega_0\Omega_{K^-};$$
$$\mu(p_\pi)=(A/2)\left[\sigma^{tot}_{\pi p}(p_\pi)+\sigma^{tot}_{\pi n}(p_\pi)\right],\quad \Theta(x_\parallel)=(x_\parallel+|x_\parallel|)/2|x_\parallel| \quad (50)$$

and

$$E'_{K^-}\frac{d\sigma_{\pi N\to K^-X}(\sqrt{s_1},\mathbf{p}'_{K^-})}{d\mathbf{p}'_{K^-}} = \frac{Z}{A}E'_{K^-}\frac{d\sigma_{\pi p\to K^-X}(\sqrt{s_1},\mathbf{p}'_{K^-})}{d\mathbf{p}'_{K^-}} +\frac{N}{A}E'_{K^-}\frac{d\sigma_{\pi n\to K^-X}(\sqrt{s_1},\mathbf{p}'_{K^-})}{d\mathbf{p}'_{K^-}}, \quad (51)$$

$$s_1=\left(E_\pi+E'_t\right)^2-\left(\mathbf{p}_\pi+\mathbf{p}'_t\right)^2, \quad (52)$$

$$E'_t = m_N-E'-C_{rec}, \quad (53)$$

$$p_\pi^{lim}(\vartheta_\pi) = \frac{\beta_Ap_0\cos\vartheta_\pi+(E_0+M_A)\sqrt{\beta_A^2-4m_\pi^2(s_A+p_0^2\sin^2\vartheta_\pi)}}{2(s_A+p_0^2\sin^2\vartheta_\pi)}, \quad (54)$$

$$\beta_A=s_A+m_\pi^2-M_{A+1}^2,\quad s_A=(E_0+M_A)^2-p_0^2. \quad (55)$$

Here, $d\sigma^{(prim)}_{pA\to\pi X}(\mathbf{p}_0)/d\mathbf{p}_\pi$ are the inclusive differential cross-sections for pion production on nuclei from the primary proton-induced reaction channel (45); $E'_{K^-}d\sigma_{\pi p\to K^-X}/d\mathbf{p}'_{K^-}$ ($E'_{K^-}d\sigma_{\pi n\to K^-X}/d\mathbf{p}'_{K^-}$) is the in-medium inclusive invariant differential cross-section for K^- production in πp(πn)-collisions *via* the subprocess (46); $\sigma^{tot}_{\pi N}(p_\pi)$ is the total cross-section of the free πN-interaction; $\mathbf{p}_\pi$ and E_π are the momentum and total energy of a pion; p_π^{abs} is the absolute threshold momentum for antikaon production on the residual nucleus by an intermediate pion ($p_\pi^{abs}\approx 1.88$ GeV/c for the production of K^--mesons with momentum of 1.28 GeV/c at a lab angle of 10.5°); $p_\pi^{lim}(\vartheta_\pi)$ is the kinematical limit for pion production at a lab angle ϑ_π from proton-nucleus collisions. The quantities $\mu(p_0)$ and $\mu(p_{K^-})$ are defined above by eq. (23). And finally the quantity C_{rec} in (53) takes properly into account the recoil energies of the residual nuclei in the two-step production process ($C_{rec}\approx 3$ and 16 MeV for initial ^{9}Be target nucleus as well as $C_{rec}\approx 0.4$ and 2 MeV for ^{63}Cu target nucleus in the case of use in (47), respectively, of uncorrelated and correlated parts of the nucleon spectral function). The in-medium momentum $\mathbf{p}'_{K^-}$ of antikaon produced in the secondary $\pi N\to NKK^-$ channel is related to the free one $\mathbf{p}_{K^-}$ by the relation (24) in which, according to the above mentioned, one has to put $m^*_{K^-}=m_K+U^0_{K^-}$ with $U^0_{K^-}=-126$ MeV.

Because we are interested in the high-momentum parts of pion spectra $\mathrm{d}\sigma^{(\mathrm{prim})}_{\mathrm{p}A\to\pi X}(\mathbf{p}_0)/\mathrm{d}\mathbf{p}_\pi$ at forward laboratory angles, as was noted above, and since the high-momentum tails of the experimental pion spectra $\mathrm{d}\sigma^{(\mathrm{exp})}_{\mathrm{p}A\to\pi X}(\mathbf{p}_0)/\mathrm{d}\mathbf{p}_\pi$ at these angles are populated mainly by the pions from first chance pN-collisions (45) [53], we will employ in our calculations of the K^- cross-sections from the two-step process (45), (46) the experimental pion yields at small angles and for high momenta. In the case of the ^{9}Be and ^{63}Cu target nuclei of interest these yields have been measured in experiment [60] at a laboratory angle of 10.5° for incident proton energies 1.75, 2.25 GeV and the results of measurements, using those from [74,75], have been parametrized as follows [60,76]:

$$E_{\pi^+}\frac{\mathrm{d}\sigma^{(\mathrm{exp})}_{\mathrm{p}^9\mathrm{Be}\to\pi^+X}(\mathbf{p}_0)}{\mathrm{d}\mathbf{p}_{\pi^+}} = 220\big(1-x_F^R\big)^{3+3p_\perp^2}\ \big[\mathrm{GeV}\cdot\mathrm{mb}/(\mathrm{GeV/c})^3\big],$$

$$E_{\pi^-}\frac{\mathrm{d}\sigma^{(\mathrm{exp})}_{\mathrm{p}^9\mathrm{Be}\to\pi^-X}(\mathbf{p}_0)}{\mathrm{d}\mathbf{p}_{\pi^-}} = 130\big(1-x_F^R\big)^{3+5p_\perp^2}\ \big[\mathrm{GeV}\cdot\mathrm{mb}/(\mathrm{GeV/c})^3\big]; \quad (56)$$

$$E_{\pi^+}\frac{\mathrm{d}\sigma^{(\mathrm{exp})}_{\mathrm{p}^{63}\mathrm{Cu}\to\pi^+X}(\mathbf{p}_0)}{\mathrm{d}\mathbf{p}_{\pi^+}} = 3650\big(x_F^R\big)^4\big(1-x_F^R\big)^{2+2x_F^R+3p_\perp^2}\ [\mathrm{GeV}\cdot\mathrm{mb}/(\mathrm{GeV/c})^3],$$

$$E_{\pi^-}\frac{\mathrm{d}\sigma^{(\mathrm{exp})}_{\mathrm{p}^{63}\mathrm{Cu}\to\pi^-X}(\mathbf{p}_0)}{\mathrm{d}\mathbf{p}_{\pi^-}} = 2460\big(x_F^R\big)^4\big(1-x_F^R\big)^{2+2.2x_F^R+5p_\perp^2}\ [\mathrm{GeV}\cdot\mathrm{mb}/(\mathrm{GeV/c})^3]; \quad (57)$$

where the radial scaling variable x_F^R is given by

$$x_F^R = \frac{\overset{*}{p}}{\overset{*}{p}_{\max}},$$

$$\overset{*}{p} = \sqrt{\overset{*}{p}_L{}^2 + p_\perp^2},$$

$$\overset{*}{p}_{\max} = \frac{1}{2\sqrt{s_A}}\lambda\big(s_A, m_\pi^2, M_{A+1}^2\big) \quad (58)$$

and $\overset{*}{p}_L, p_\perp$ are the longitudinal and transverse momenta of pion in the pA center-of-mass system, respectively; $\overset{*}{p}_{\max}$ is the maximum value of $\overset{*}{p}$ allowed by the kinematics. The quantity s_A is defined above by eq. (55). The π^0 spectrum also needed for our calculations can be approximately expressed *via* the $\pi^\pm$ spectra as

$$E_{\pi^0}\frac{\mathrm{d}\sigma^{(\mathrm{exp})}_{\mathrm{p}A\to\pi^0X}(\mathbf{p}_0)}{\mathrm{d}\mathbf{p}_{\pi^0}} = \frac{1}{2}\left[E_{\pi^+}\frac{\mathrm{d}\sigma^{(\mathrm{exp})}_{\mathrm{p}A\to\pi^+X}(\mathbf{p}_0)}{\mathrm{d}\mathbf{p}_{\pi^+}} + E_{\pi^-}\frac{\mathrm{d}\sigma^{(\mathrm{exp})}_{\mathrm{p}A\to\pi^-X}(\mathbf{p}_0)}{\mathrm{d}\mathbf{p}_{\pi^-}}\right]. \quad (59)$$

In our method the Lorentz invariant inclusive cross-section for K^- production in πN-collisions (46) has been described by the three-body phase space calculations normalized to the respective "in-medium" total cross-section $\sigma_{\pi\mathrm{N}\to\mathrm{NKK}^-}(\sqrt{s_1}, \sqrt{s^*_{1,\mathrm{th}}})$. According to [77], one has

$$E'_{\mathrm{K}^-}\frac{\mathrm{d}\sigma_{\pi\mathrm{N}\to\mathrm{NKK}^-}(\sqrt{s_1}, \mathbf{p}'_{\mathrm{K}^-})}{\mathrm{d}\mathbf{p}'_{\mathrm{K}^-}} = \frac{\pi}{4}\frac{\sigma_{\pi\mathrm{N}\to\mathrm{NKK}^-}\big(\sqrt{s_1}, \sqrt{s^*_{1,\mathrm{th}}}\big)}{I_3\big(s_1, m^*_{\mathrm{K}^+}, m^*_{\mathrm{K}^-}, m^*_{\mathrm{N}}\big)}\frac{\lambda\big(s_{\mathrm{KN}}, m^{*2}_{\mathrm{K}^+}, m^{*2}_{\mathrm{N}}\big)}{s_{\mathrm{KN}}}, \quad (60)$$

$$s_{\mathrm{KN}} = s_1 + m^{*2}_{\mathrm{K}^-} - 2\big(E_\pi + E'_{\mathrm{t}}\big)E'_{\mathrm{K}^-} + 2(\mathbf{p}_\pi + \mathbf{p}'_{\mathrm{t}})\mathbf{p}'_{\mathrm{K}^-} \quad (61)$$

and

$$\sqrt{s^*_{1,\mathrm{th}}} = \sqrt{s_{1,\mathrm{th}}} + U^0_{\mathrm{N}} + U^0_{\mathrm{K}^+} + U^0_{\mathrm{K}^-}, \quad (62)$$

where $\sqrt{s_{1,\mathrm{th}}} = m_{\mathrm{N}} + 2m_{\mathrm{K}}$ is the vacuum threshold energy and the quantities I_3, λ are defined by the (27), (29), respectively. Like above, we assume that the "in-medium" cross-section $\sigma_{\pi\mathrm{N}\to\mathrm{NKK}^-}(\sqrt{s_1}, \sqrt{s^*_{1,\mathrm{th}}})$ is equivalent to the vacuum cross-section $\sigma_{\pi\mathrm{N}\to\mathrm{NKK}^-}(\sqrt{s_1}, \sqrt{s_{1,\mathrm{th}}})$ in which the free threshold $\sqrt{s_{1,\mathrm{th}}}$ is replaced by the effective threshold $\sqrt{s^*_{1,\mathrm{th}}}$ as given by eq. (62). For the free total cross-section $\sigma_{\pi\mathrm{N}\to\mathrm{NKK}^-}(\sqrt{s_1}, \sqrt{s_{1,\mathrm{th}}})$ we have used the following parametrization suggested in [77]:

$$\sigma_{\pi\mathrm{N}\to\mathrm{NKK}^-}(\sqrt{s_1}, \sqrt{s_{1,\mathrm{th}}}) = \frac{A[(\sqrt{s_1} - \sqrt{s_{1,\mathrm{th}}})/\,\mathrm{GeV}]^i}{B + \big[\big(\sqrt{s_1} - \sqrt{s_{1,\mathrm{th}}}\big)/\,\mathrm{GeV}\big]^j}, \quad (63)$$

where the constants A, B, i and j are given in table 1.

For obtaining the total cross-sections of $\pi^0\mathrm{p} \to \mathrm{pK}^+\mathrm{K}^-$, $\pi^0\mathrm{n} \to \mathrm{nK}^+\mathrm{K}^-$ and $\pi^0\mathrm{n} \to \mathrm{pK}^0\mathrm{K}^-$ reactions where data are not available we have employed the isospin considerations. They have shown that there exist the following relations[5] among the $\sigma'_{\pi\mathrm{N}\to\mathrm{NKK}^-}s$:

$$2\sigma_{\pi^-\mathrm{p}\to\mathrm{nK}^+\mathrm{K}^-} + \sigma_{\pi^-\mathrm{n}\to\mathrm{nK}^0\mathrm{K}^-} + \sigma_{\pi^-\mathrm{p}\to\mathrm{pK}^0\mathrm{K}^-} = 2\big[2\sigma_{\pi^0\mathrm{p}\to\mathrm{pK}^+\mathrm{K}^-} + \sigma_{\pi^0\mathrm{n}\to\mathrm{pK}^0\mathrm{K}^-}\big], \quad (64)$$

$$\sigma_{\pi^0\mathrm{p}\to\mathrm{pK}^+\mathrm{K}^-} = \sigma_{\pi^0\mathrm{n}\to\mathrm{nK}^+\mathrm{K}^-} \quad (65)$$

and

$$\sigma_{\pi^0\mathrm{n}\to\mathrm{pK}^0\mathrm{K}^-} \approx \sigma_{\pi^-\mathrm{p}\to\mathrm{nK}^+\mathrm{K}^-}. \quad (66)$$

Using (64)–(66), one gets

$$\sigma_{\pi^0\mathrm{p}\to\mathrm{pK}^+\mathrm{K}^-} = \sigma_{\pi^0\mathrm{n}\to\mathrm{nK}^+\mathrm{K}^-} = \frac{1}{4}\big(\sigma_{\pi^-\mathrm{n}\to\mathrm{nK}^0\mathrm{K}^-} + \sigma_{\pi^-\mathrm{p}\to\mathrm{pK}^0\mathrm{K}^-}\big). \quad (67)$$

Within the representation (60), the inclusive invariant differential cross-sections $E'_{\mathrm{K}^-}\mathrm{d}\sigma_{\pi\mathrm{p}\to\mathrm{K}^-X}/\mathrm{d}\mathbf{p}'_{\mathrm{K}^-}$ and

[5] It should be noted that these relations are in line with those among the $\sigma'_{\pi\mathrm{N}\to\mathrm{NKK}^-}s$ derived in [78] employing the K*-resonance exchange model.

Table 1. Parameters in the approximation of the partial cross-sections for the production of K^--mesons in πN-collisions

Reaction	A (mb)	B	i	j
$\pi^+ + n \to p + K^+ + K^-$	0.1757	0.4938	1	2
$\pi^- + p \to n + K^+ + K^-$	0.1800	0.0549	2	3
$\pi^- + p \to p + K^0 + K^-$	0.0576	0.0549	2	3
$\pi^- + n \to n + K^0 + K^-$	0.0647	0.2910	1	2

$E'_{K^-}\mathrm{d}\sigma_{\pi n\to K^- X}/\mathrm{d}\mathbf{p}'_{K^-}$ for antikaon production in πp- and πn-interactions appearing in eq. (51) can be written in the following forms:

$$
\begin{aligned}
&E'_{K^-}\frac{\mathrm{d}\sigma_{\pi^+ p\to K^- X}(\sqrt{s_1},\mathbf{p}'_{K^-})}{\mathrm{d}\mathbf{p}'_{K^-}}=0,\\
&E'_{K^-}\frac{\mathrm{d}\sigma_{\pi^+ n\to K^- X}(\sqrt{s_1},\mathbf{p}'_{K^-})}{\mathrm{d}\mathbf{p}'_{K^-}}=\\
&\quad E'_{K^-}\frac{\mathrm{d}\sigma_{\pi^+ n\to pK^+K^-}(\sqrt{s_1},\mathbf{p}'_{K^-})}{\mathrm{d}\mathbf{p}'_{K^-}};
\end{aligned}
\tag{68}
$$

$$
\begin{aligned}
&E'_{K^-}\frac{\mathrm{d}\sigma_{\pi^0 p\to K^- X}(\sqrt{s_1},\mathbf{p}'_{K^-})}{\mathrm{d}\mathbf{p}'_{K^-}}=\\
&\quad E'_{K^-}\frac{\mathrm{d}\sigma_{\pi^0 p\to pK^+K^-}(\sqrt{s_1},\mathbf{p}'_{K^-})}{\mathrm{d}\mathbf{p}'_{K^-}},\\
&E'_{K^-}\frac{\mathrm{d}\sigma_{\pi^0 n\to K^- X}(\sqrt{s_1},\mathbf{p}'_{K^-})}{\mathrm{d}\mathbf{p}'_{K^-}}=\\
&\quad E'_{K^-}\frac{\mathrm{d}\sigma_{\pi^0 n\to nK^+K^-}(\sqrt{s_1},\mathbf{p}'_{K^-})}{\mathrm{d}\mathbf{p}'_{K^-}}\\
&\quad +E'_{K^-}\frac{\mathrm{d}\sigma_{\pi^0 n\to pK^0K^-}(\sqrt{s_1},\mathbf{p}'_{K^-})}{\mathrm{d}\mathbf{p}'_{K^-}};
\end{aligned}
\tag{69}
$$

$$
\begin{aligned}
&E'_{K^-}\frac{\mathrm{d}\sigma_{\pi^- p\to K^- X}(\sqrt{s_1},\mathbf{p}'_{K^-})}{\mathrm{d}\mathbf{p}'_{K^-}}=\\
&\quad E'_{K^-}\frac{\mathrm{d}\sigma_{\pi^- p\to nK^+K^-}(\sqrt{s_1},\mathbf{p}'_{K^-})}{\mathrm{d}\mathbf{p}'_{K^-}}\\
&\quad +E'_{K^-}\frac{\mathrm{d}\sigma_{\pi^- p\to pK^0K^-}(\sqrt{s_1},\mathbf{p}'_{K^-})}{\mathrm{d}\mathbf{p}'_{K^-}},\\
&E'_{K^-}\frac{\mathrm{d}\sigma_{\pi^- n\to K^- X}(\sqrt{s_1},\mathbf{p}'_{K^-})}{\mathrm{d}\mathbf{p}'_{K^-}}=\\
&\quad E'_{K^-}\frac{\mathrm{d}\sigma_{\pi^- n\to nK^0K^-}(\sqrt{s_1},\mathbf{p}'_{K^-})}{\mathrm{d}\mathbf{p}'_{K^-}}.
\end{aligned}
\tag{70}
$$

Let us now simplify expression (47) describing the invariant differential cross-section for K^- production in pA-collisions *via* the two-step process. Considering that the main contribution to the cross-section for antikaon production at forward laboratory angles comes from fast pions moving in the beam direction and that the πN total cross-section $\sigma^{\mathrm{tot}}_{\pi N}$ in the energy region of interest is approximately constant with a magnitude of $\langle\sigma^{\mathrm{tot}}_{\pi N}\rangle\approx 35$ mb [52], we can recast this expression into the form

$$
\begin{aligned}
&E_{K^-}\frac{\mathrm{d}\sigma^{(\mathrm{sec})}_{pA\to K^- X}(\mathbf{p}_0)}{\mathrm{d}\mathbf{p}_{K^-}}=\\
&\frac{I_V\left[A,\sigma^{\mathrm{in}}_{pN}(p_0),\langle\sigma^{\mathrm{tot}}_{\pi N}\rangle,\sigma^{\mathrm{tot}}_{K^-N}(p_{K^-}),0^0,0^0\right]}{I'_V\left[A,\sigma^{\mathrm{in}}_{pN}(p_0),\langle\sigma^{\mathrm{tot}}_{\pi N}\rangle,0^0\right]}\\
&\times\sum_{\pi=\pi^+,\pi^0,\pi^-}\int_{4\pi}\mathrm{d}\Omega_\pi\int_{p^{\mathrm{abs}}_\pi}^{p^{\lim}_\pi(\vartheta_\pi)}p_\pi^2\,\mathrm{d}p_\pi\frac{\mathrm{d}\sigma^{(\mathrm{prim})}_{pA\to\pi X}(\mathbf{p}_0)}{\mathrm{d}\mathbf{p}_\pi}\\
&\times\iint P(\mathbf{p}'_t,E')\mathrm{d}\mathbf{p}'_t\,\mathrm{d}E'\\
&\quad\times\left[E'_{K^-}\frac{\mathrm{d}\sigma_{\pi N\to K^- X}(\sqrt{s_1},\mathbf{p}'_{K^-})}{\mathrm{d}\mathbf{p}'_{K^-}}\right],
\end{aligned}
\tag{71}
$$

where according to (52)

$$
s_1=\left(E_\pi+E'_t\right)^2-\left(p_\pi\Omega_{\mathbf{0}}+\mathbf{p}'_t\right)^2. \tag{72}
$$

For a nucleus of radius $R=1.3\cdot A^{1/3}$ fm and with a uniform nucleon density, the expressions for $I_V[A,\sigma^{\mathrm{in}}_{pN}(p_0),\langle\sigma^{\mathrm{tot}}_{\pi N}\rangle,\sigma^{\mathrm{tot}}_{K^-N}(p_{K^-}),0^0,0^0]$ and $I'_V[A,\sigma^{\mathrm{in}}_{pN}(p_0),\langle\sigma^{\mathrm{tot}}_{\pi N}\rangle,0^0]$ are reduced to the following simple forms:

$$
\begin{aligned}
&I_V\left[A,\sigma^{\mathrm{in}}_{pN}(p_0),\langle\sigma^{\mathrm{tot}}_{\pi N}\rangle,\sigma^{\mathrm{tot}}_{K^-N}(p_{K^-}),0^\circ,0^\circ\right]=\\
&\quad\frac{9A^2}{2\pi R^2(a_2-a_3)}\left[I(a_1,a_3)-I(a_1,a_2)\right],
\end{aligned}
\tag{73}
$$

$$
\begin{aligned}
&I(a_1,a)=\frac{1}{(a_1-a)}\\
&\quad\times\left\{\frac{1}{a^2}\left[1-(1+a)e^{-a}\right]-\frac{1}{a_1^2}\left[1-(1+a_1)e^{-a_1}\right]\right\};
\end{aligned}
\tag{74}
$$

$$
\begin{aligned}
&I'_V\left[A,\sigma^{\mathrm{in}}_{pN}(p_0),\langle\sigma^{\mathrm{tot}}_{\pi N}\rangle,0^0\right]=\frac{3A}{(a_3-a_2)a_2^2}\\
&\times\left\{1-(1+a_2)e^{-a_2}-\left(\frac{a_2}{a_3}\right)^2\left[1-(1+a_3)e^{-a_3}\right]\right\},
\end{aligned}
\tag{75}
$$

where $a_1=3\mu(p_{K^-})/2\pi R^2$, $a_2=3\mu(p_0)/2\pi R^2$ and $a_3=3A\langle\sigma^{\mathrm{tot}}_{\pi N}\rangle/2\pi R^2$. In the case of $a_1=a_2$ relevant for the kinematical conditions of the experiment [60] (see, (41)) the quantity $I(a_1,a_2)$, entering into eq. (73), can be put in view of eq. (74) in a simpler form

$$
I(a_1,a_2=a_1)=I(a_1)=\frac{2}{a_1^3}\left[1-\left(1+a_1+\frac{a_1^2}{2}\right)e^{-a_1}\right]. \tag{76}
$$

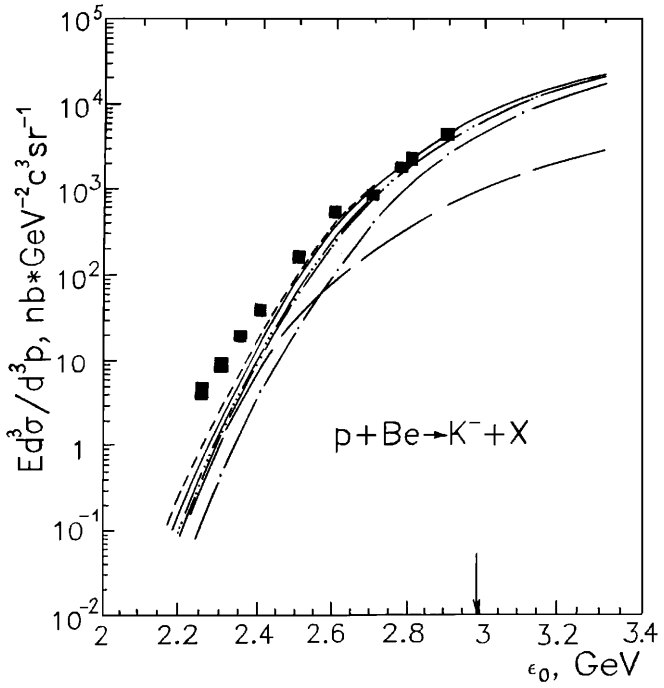

Fig. 2. Lorentz invariant cross-sections for the production of K^--mesons with momentum of 1.28 GeV/c at a lab angle of 10.5° in p + ^{9}Be reactions as functions of the laboratory kinetic energy ϵ_0 of the proton. The experimental data (full squares) are from the experiment [60]. The curves are our calculation with the density-dependent potentials. The dashed lines with one, two, three dots; the solid and short-dashed lines are calculations for primary production process (1) with the total nucleon spectral function at $V_0 = 40$ MeV, $U_N(\rho_N) = 0$, $U_{K^+}(\rho_N) = 0$, $U_{K^-}(\rho_N) = 0$; $V_0 = 40$ MeV, $U_N(\rho_N) = -34(\rho_N/\rho_0)$ MeV, $U_{K^+}(\rho_N) = 22(\rho_N/\rho_0)$ MeV, $U_{K^-}(\rho_N) = -126(\rho_N/\rho_0)$ MeV; $V_0 = 40$ MeV, $U_N(\rho_N) = -34(\rho_N/\rho_0)$ MeV, $U_{K^+}(\rho_N) = 0$, $U_{K^-}(\rho_N) = 0$; $V_0 = 40$ MeV, $U_N(\rho_N) = -34(\rho_N/\rho_0)$ MeV, $U_{K^+}(\rho_N) = 0$, $U_{K^-}(\rho_N) = -126(\rho_N/\rho_0)$ MeV and $V_0 = 40$ MeV, $U_N(\rho_N) = -50(\rho_N/\rho_0)$ MeV, $U_{K^+}(\rho_N) = 0$, $U_{K^-}(\rho_N) = 0$, respectively. The long-dashed line denotes the same as the dashed line with two dots, but it is supposed in addition that the total nucleon spectral function is replaced by its correlated part. The arrow indicates the threshold for the reaction pN → NNKK$^-$ occurring on a free nucleon at the kinematics under consideration.

Finally, it is interesting to note that in the case of $a_1 = a_2 = a_3$, which is realistic enough as well, the expression (73) can be reduced to a substantially more simple form, viz.:

$$I_V\left[A, \sigma_{pN}^{in}(p_0), \langle\sigma_{\pi N}^{tot}\rangle, \sigma_{K^-N}^{tot}(p_{K^-}), 0°, 0°\right] = \frac{9A^2}{4\pi a_1 R^2}\left[3I(a_1) - e^{-a_1}\right], \quad (77)$$

where the quantity $I(a_1)$ is defined above by eq. (76).

Now, let us discuss the results of our calculations for antikaon production in pBe- and pCu-interactions in the framework of model outlined above.

3 Results and discussion

At first, we will concentrate on the results of our calculations for the direct K^- production mechanism.

Figure 2 shows a comparison of the calculated invariant cross-section by (36), (41)–(44) for the production of K^--mesons with momentum of 1.28 GeV/c at a laboratory angle of 10.5° from primary pN → NNKK$^-$ channel with the data from the experiment [60] for p + ^{9}Be → K^- + X reaction at the various bombarding energies. One can see that

1) our model for primary antikaon production process, based on nucleon spectral function, fails completely (especially at "low" beam energies, dash-dotted line) to reproduce the experimental data at subthreshold beam energies (at energies ≤ 2.99 GeV for the kinematical conditions of the experiment [60]) without allowance for the influence of the corresponding nuclear mean-field potentials on the one-step production process (1);
2) a simultaneous inclusion of potentials for final nucleons, kaon and antikaon (dashed line with two dots) leads to an enhancement of the K^- yield by about a factors of 1.6 and 3, respectively, at "high" and "low" incident energies as well as to a reasonably good description of the experimental data except for the four lowest data points;
3) the previous scenario is hardly distinguishable from the one with employing only the attractive outgoing nucleon effective potential (dashed line with three dots), which indicates that the simultaneous application of kaon and antikaon potentials unaffects the K^- yield and it is mainly governed by the nucleon mean-field potential;
4) although the K^+ and K^- potentials are substantially different in magnitude, the effect of the K^+ potential alone (compare solid line and dashed line with two dots) is comparable to that from the K^- potential alone (compare solid line and dashed line with three dots) and they act in opposite directions, namely, the inclusion of the K^+ or K^- potential alone results in reduction or enhancement of the antikaon yield by a factors of about 1.2 and 1.5, respectively, at "high" and "low" beam energies which are insufficient to describe the data in case when only antikaon potential alone is included;
5) our calculations with including simultaneously both attractive antikaon (4), (5) and nucleon (8), (9) effective potentials (solid line in fig. 2) reproduce quite well the experimental data in the energy region[6] $\epsilon_0 \geq$ 2.4 GeV, but nevertheless underestimate the data at lower bombarding energies as in the cases considered above with the different scenarios for the in-medium

[6] This counts in favour of the scenario that for positive charged kaons apparently not any medium modifications are needed to reproduce the data in this energy region.

masses of hadrons produced in the primary production process (1)[7];

6) an application of the effective nucleon potential (8), (10) alone (short-dashed line) leads to a result which gives also a rather good description of the experimental data except for the three lowest data points, what means, taking into account the above mentioned, that the determination of the K^- potential from the excitation function for "hard" antikaons appears to be difficult;
7) the antikaon yield from the one-step K^- production mechanism is entirely governed by the correlated part of the nucleon spectral function only in the far subthreshold energy region (at bombarding energies of $\epsilon_0 \leq 2.4\,\mathrm{GeV}$), which intimates that internal nucleon momenta greater than the Fermi momentum are needed for K^- production in direct process (1) at given kinematics and at these beam energies[8].

The results presented in fig. 2 indicate, as was also noted above, that the one-step production process (1) misses the experimental data in the energy region far below the free threshold (at beam energies $\epsilon_0 \leq 2.4\,\mathrm{GeV}$) even when the influence of the nuclear density-dependent mean-field potentials (4)–(6), (8)–(10) has been included. But the K^- creation due to first chance pN-collisions (1) in this energy region occurs, as is evident from the foregoing, when the incident protons collide with the short-range two-nucleon (or multinucleon) correlations inside the target nucleus, and this means that the local baryon density around the spatial creation points of hadrons in these collisions can be high [54]. Therefore, the antikaon production in the far subthreshold energy region should be evaluated more likely for the density-independent potentials with depths (5) and (9) taken at normal nuclear density ρ_0 than for the density-dependent fields (4) and (8) where the local average nuclear density is involved.

The results of such calculations obtained both for the one-step (1) and two-step (45), (46) reaction channels as well as the same experimental data as those presented in fig. 2 are shown in fig. 3. It is seen that

1) our calculations for the one-step reaction channel (1) with the set of parameters $V_0 = 40\,\mathrm{MeV}$, $U_\mathrm{N}^0 = 0$, $U_{\mathrm{K}^+}^0 = 22\,\mathrm{MeV}$, $U_{\mathrm{K}^-}^0 = -126\,\mathrm{MeV}$ (dot-dashed line) substantially underpredict the data in the energy region far below the threshold, whereas the additional inclusion of the nucleon effective potential $U_\mathrm{N}^0 = -34\,\mathrm{MeV}$ (dashed line with two dots) leads to a quite good description of the data in this energy region, and this means that the K^- yield is almost totally determined by the nucleon mean-field potential (compare as well dashed lines with two and three dots in fig. 3);
2) the scenario when only attractive antikaon density-independent potential with depth $U_{\mathrm{K}^-}^0 = -126\,\mathrm{MeV}$ alone is used does not allow us to reproduce the data in the far subthreshold energy region (compare solid line and dashed line with three dots), which is in line with our findings inferred above from the analysis of the same data with the density-dependent potentials;
3) the results of our calculations of the antikaon yield from the secondary reaction channel (46) with including the influence of the different in-medium scenarios

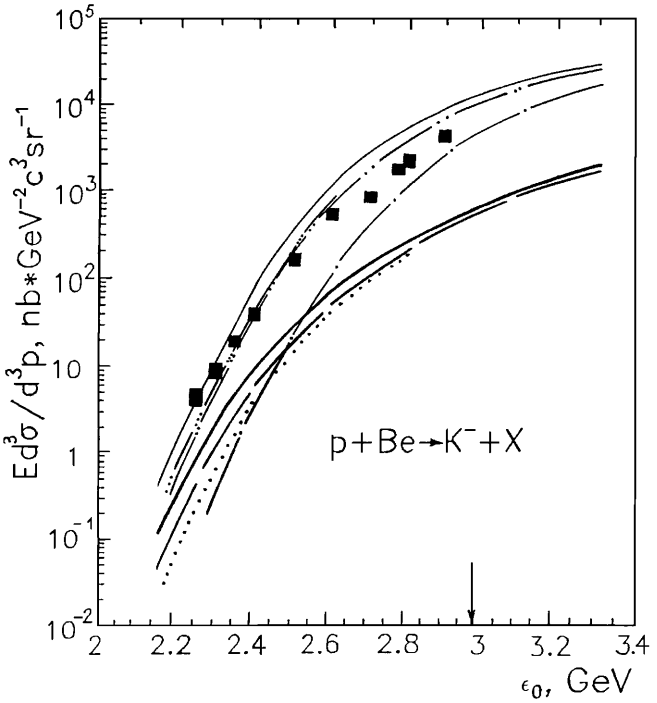

Fig. 3. Lorentz invariant cross-sections for the production of K^--mesons with momentum of 1.28 GeV/c at a lab angle of 10.5° in p + ^{9}Be reactions as functions of the laboratory energy of the proton. The experimental data (full squares) are from the experiment [60]. The curves are our calculation with the density-independent potentials. The dashed lines with one, two, three dots and the thin solid line are calculations for primary production process (1) with the total nucleon spectral function at $V_0 = 40\,\mathrm{MeV}$, $U_\mathrm{N}^0 = 0$, $U_{\mathrm{K}^+}^0 = 22\,\mathrm{MeV}$, $U_{\mathrm{K}^-}^0 = -126\,\mathrm{MeV}$; $V_0 = 40\,\mathrm{MeV}$, $U_\mathrm{N}^0 = -34\,\mathrm{MeV}$, $U_{\mathrm{K}^+}^0 = 22\,\mathrm{MeV}$, $U_{\mathrm{K}^-}^0 = -126\,\mathrm{MeV}$; $V_0 = 40\,\mathrm{MeV}$, $U_\mathrm{N}^0 = -34\,\mathrm{MeV}$, $U_{\mathrm{K}^+}^0 = 0$, $U_{\mathrm{K}^-}^0 = 0$ and $V_0 = 40\,\mathrm{MeV}$, $U_\mathrm{N}^0 = -34\,\mathrm{MeV}$, $U_{\mathrm{K}^+}^0 = 0$, $U_{\mathrm{K}^-}^0 = -126\,\mathrm{MeV}$, respectively. The dotted, long-dashed and thick solid lines are calculations by (71)–(76) for the secondary production process (46) at $U_\mathrm{N}^0 = 0$, $U_{\mathrm{K}^+}^0 = 0$, $U_{\mathrm{K}^-}^0 = 0$; $U_\mathrm{N}^0 = -34\,\mathrm{MeV}$, $U_{\mathrm{K}^+}^0 = 22\,\mathrm{MeV}$, $U_{\mathrm{K}^-}^0 = -126\,\mathrm{MeV}$ and $U_\mathrm{N}^0 = -34\,\mathrm{MeV}$, $U_{\mathrm{K}^+}^0 = 0$, $U_{\mathrm{K}^-}^0 = -126\,\mathrm{MeV}$, respectively. The arrow indicates the threshold for the reaction $\mathrm{pN} \to \mathrm{NNKK}^-$ occuring on a free nucleon at the kinematics under consideration.

[7] It should be pointed out that the use in the calculation the K^- optical potential (6), extracted from the kaonic atom data, instead of potential (4), (5) leads to an increase of the "low" energy ($\epsilon_0 \leq 2.5\,\mathrm{GeV}$) and "high" energy ($\epsilon_0 > 2.5\,\mathrm{GeV}$) parts of the antikaon excitation function only by about 15% and 5%, respectively.

[8] Calculations show that the minimal internal nucleon momenta needed for K^- production in primary process (1) at incident energies of 2.25, 2.30, 2.35 and 2.40 GeV corresponding to the four lowest data points in fig. 2, respectively, are 424, 374, 331 and 291 MeV/c.

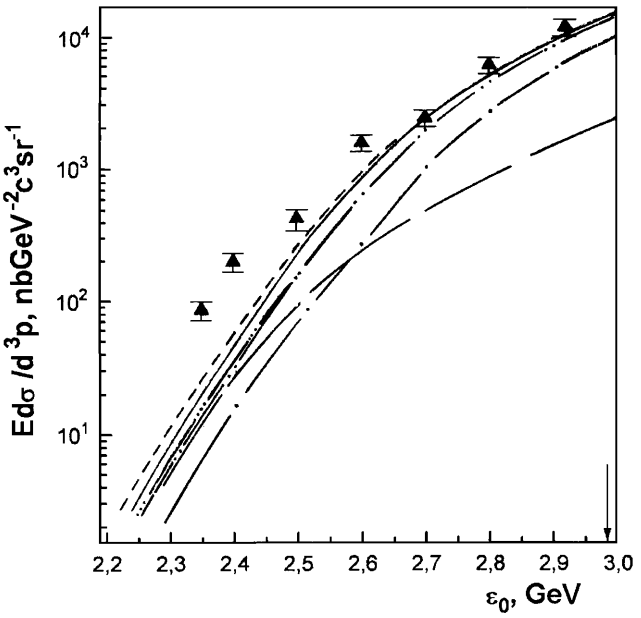

Fig. 4. Lorentz invariant cross-sections for the production of K^--mesons with momentum of 1.28 GeV/c at a lab angle of 10.5° in p + ^{63}Cu reactions as functions of the laboratory energy of the proton. The experimental data (full triangles) are from the experiment [60]. The curves are our calculation with the density-dependent potentials. The notation of the curves is identical to that in fig 2. The arrow indicates the threshold for the reaction pN → NNKK$^-$ occuring on a free nucleon at the kinematics under consideration.

on it underestimate[9] essentially the data and calculated cross-sections from primary process (1) (dashed lines with two and three dots, solid line), which implies the dominance of the one-step K^- production mechanism for the considered antikaon production at all beam energies of interest.

Let us consider now the subthreshold K^- production from p + ^{63}Cu reactions within the above model.

Figure 4 presents measured and calculated by (36), (41)–(43) invariant cross-sections for the production of K^--mesons with momentum of 1.28 GeV/c at the laboratory angle of 10.5° from primary pN → NNKK$^-$ channel in p^{63}Cu-reactions at different bombarding energies. It is clearly seen that

1) only a simultaneous inclusion attractive antikaon (4), (5) and nucleon (8), (9) effective potentials (solid line in fig. 4) or an application of the nucleon potential (8), (10) alone (short-dashed line) allows us to describe rather well the experimental data except for the two lowest data points, what is consistent with our previous findings of fig. 2;
2) employing only the attractive outgoing nucleon potential (8), (9) leads to an enhancement of the K^- yield by about a factors of 2.5 and 1.5, respectively, at 2.5 and 2.9 GeV beam energies, whereas the additional inclusion of the K^- potential (4), (5) alone results in enlargement of the antikaon yield yet by a factors of about 1.5 and 1.1 at these energies, which indicates that the effect of the nucleon mean-field is of importance in explaining the experimental data on "hard" antikaon production at considered incident energies and the influence of the K^- optical potential alone is insufficient to describe the data under consideration;
3) a simultaneous application of kaon and antikaon potentials unaffects practically the K^- yield (compare dashed lines with two and three dots) as in the discussed above case of the K^- production on ^{9}Be target nucleus;
4) the main contribution to the K^- production in the far subthreshold energy region (at beam energies $\epsilon_0 \leq$ 2.4 GeV) comes from the use in our calculations with the density-dependent mean-field potentials only of the correlated part of the nucleon spectral function (long-dashed line), which means in line with the conclusion drawn above from the analysis of the K^- data from p^{9}Be-interactions that the antikaon production in this energy region should be evaluated for the density-independent potentials rather than for the density-dependent fields.

The results of such calculations performed for the one-step (1) and two-step (45), (46) reaction channels as well as the same experimental data as those presented in fig. 4 are given in fig. 5. It is nicely seen that

1) our calculations for the one-step reaction channel (1) with the set of parameters $V_0 = 40$ MeV, $U_{\rm N}^0 = 0$, $U_{\rm K^+}^0 = 22$ MeV, $U_{\rm K^-}^0 = -126$ MeV (dot-dashed line) miss essentially the data in the energy region $\epsilon_0 \leq$ 2.6 GeV, whereas the additional inclusion of the nucleon effective potential $U_{\rm N}^0 = -34$ MeV (dashed line with two dots) leads to a fairly good description of the data at 2.5 and 2.6 GeV incident energies as well as to a much better description of the two lowest data points compared both to the previous one and to that obtained with adopting the corresponding density-dependent potentials (cf. fig. 4);
2) the scenario when only attractive nucleon and antikaon density-independent potentials with depths $U_N^0 = -34$ MeV and $U_{\rm K^-}^0 = -126$ MeV are used (solid line) allows us to reproduce quite well these data points, and this counts also in favour of the conclusion deduced above that for positive charged kaons apparently no any medium modifications are needed to explain the data under consideration;
3) an application of only antikaon density-independent potential with depth $U_{\rm K^-}^0 = -126$ MeV alone does not allow us to describe the data at energies far below the free K^- production threshold (compare solid line and dashed line with three dots) and the K^- yield is mainly determined by the nucleon mean-field potential, and this is in line with our findings of figs. 2–4;
4) the two-step to one-step antikaon creation cross-section ratio calculated with allowance for the influ-

[9] Thus, for example, the two-step (thick solid line) to one-step (thin solid line) K^- production cross-section ratio is about 1/5 at "low" kinetic energies ($\epsilon_0 \approx$ 2.2–2.3 GeV) and about 1/20 at "high" beam energies ($\epsilon_0 \approx$ 2.7–2.9 GeV).

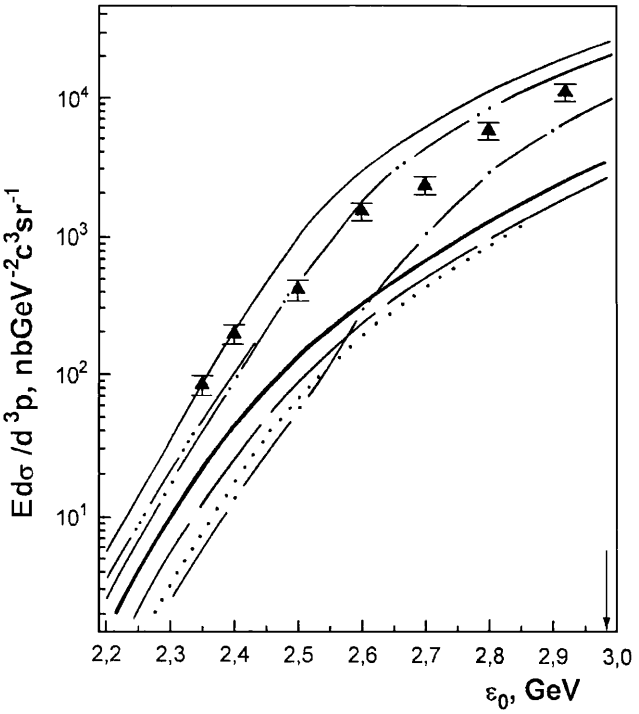

Fig. 5. Lorentz invariant cross-sections for the production of K^--mesons with momentum of 1.28 GeV/c at a lab angle of 10.5° in p + ^{63}Cu reactions as functions of the laboratory energy of the proton. The experimental data (full triangles) are from the experiment [60]. The curves are our calculation with the density-independent potentials. The notation of the curves is identical to that in fig. 3. The arrow indicates the threshold for the reaction $pN \to NNKK^-$ occuring on a free nucleon at the kinematics under consideration.

ence of the same nuclear mean fields on hadrons produced in secondary (46) and primary (1) reaction channels (thick and thin solid lines, long-dashed line and dashed line with two dots in fig. 5) is about 1/3 and 1/10, respectively, at "low" and "high" bombarding energies, which indicates that, as in the case of ^{9}Be target nucleus considered above (see, fig. 3), the one-step K^- production mechanism also dominates in the subthreshold "hard" antikaon production in p^{63}Cu-collisions [60].

It should be emphasized that the latter is in line with the findings inferred in [53] relatively to the role played by the direct K^+ production mechanism in the subthreshold kaon creation in p^{9}Be-interactions in the same kinematical conditions [54,55,58] as those used in the experiment [60]. Therefore, the reaction $p + A \to K^- + X$ in the subthreshold regime and for "hard" kinematics along with the $p + A \to K^+ + X$ one may be recommended for experimental study of the high-momentum components within target nucleus.

Taking into account what considered above, one may conclude that the determination of the K^- potential in nuclear matter from the measurements of the primary-proton energy dependence of the double differential cross-sections for production of "hard" antikaons on light and medium target nuclei in the subthreshold energy regime appears to be difficult. On the other hand, the recent studies [23,58] of the subthreshold and near threshold K^- production in pA-reactions, carried out within a coupled transport approach [23] and a simple folding model [58] based on the internal nucleon momentum distribution, indicate that the K^- potential has a strong effect on the K^- yields at low antikaon momenta. Therefore, it is interesting to explore the sensitivity of the "soft" (low momentum) K^- production in pA-interactions at subthreshold incident energies to the medium effects considered by us in the framework of the approach outlined above.

Figure 6 shows invariant cross-sections calculated by (36)–(40) for the production of K^--mesons with momentum of 0.4 GeV/c at a laboratory angle of 10.5° from primary $pN \to NNKK^-$ reaction channel in p^{9}Be-collisions at different beam energies. The nucleon, kaon and antikaon effective potentials in the calculations were assumed to be density-independent. The elementary cross-sections $\sigma^{tot}_{K^-p}$ and $\sigma^{tot}_{K^-n}$ at $p_{K^-} = 0.4$ GeV/c, needed for our calculations, were borrowed from [20,61]. It can be seen that, contrary to the case of the "hard" antikaon production discussed above, the K^- potential has a dramatic effect on the antikaon excitation function at all subthreshold energies (compare solid line and dashed line with three dots in fig. 6), which is approximately the same as that from nucleon effective potential (compare dashed line with three dots and dashed line) in the energy region $1.6\,\text{GeV} \le \epsilon_0 \le 2.0\,\text{GeV}$ and even greater than the latter at $\epsilon_0 > 2.0$ GeV. While the kaon potential has a minor effect on the K^- yield at incident energies $\epsilon_0 > 2.0$ GeV (compare solid line and dashed line with two dots), at lower beam energies it reduces the K^- production cross-section by a factor of about 2–2.5. As a result, the sensitivity to kaon and antikaon potentials (compare dot-dashed and dashed lines) is greater than that to nucleon mean field at kinetic energies > 2 GeV, whereas at lower bombarding energies the effect of nucleon potential is dominant. It is apparent that at least the former case opens an opportunity to determine the K^- potential in nuclear matter experimentally.

Finally, fig. 7 presents double differential cross-sections calculated by (36)–(40) for the production of K^--mesons from primary $pN \to NNKK^-$ channel at a laboratory angle of 10° in the interaction of protons with energy of 2.3 GeV with ^{12}C nuclei. As in the calculations of fig. 6, the nucleon, kaon and antikaon effective potentials were assumed to be density-independent. The nucleon spectral function for ^{12}C target nucleus was taken from [52]. We have employed also in our calculations of the K^- production cross-sections on ^{12}C nuclei the value of $0.358\,\text{fm}^{-2}$ for the parameter b entering into the density distribution (34). It is clearly seen that the low-momentum part ($p_{lab} \le 0.4$ GeV/c) of the K^- spectrum is almost completely determined by the antikaon potential, whereas the nucleon and kaon optical potentials play here a minor role. Its high-momentum part ($p_{lab} \ge 0.8$ GeV/c) is almost entirely governed by the nucleon effective potential, which is consistent with our previous findings of figs. 2–5.

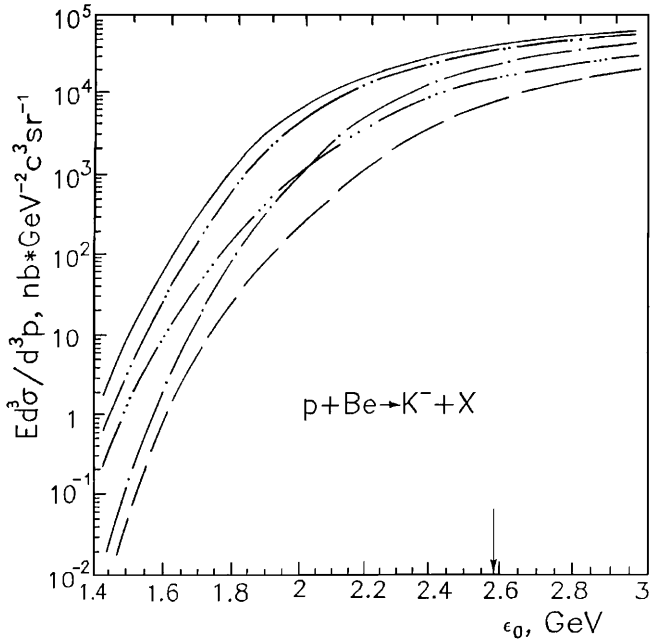

Fig. 6. Lorentz invariant cross-sections for the production of K^--mesons with momentum of 0.4 GeV/c at a lab angle of 10.5° in p + ^{9}Be reactions as functions of the laboratory energy of the proton. The dashed line is calculation for primary production process (1) with the total nucleon spectral function at $V_0 = 40$ MeV, $U_N^0 = 0$, $U_{K+}^0 = 0$, $U_{K-}^0 = 0$. The rest of notation is identical to that in fig. 3.

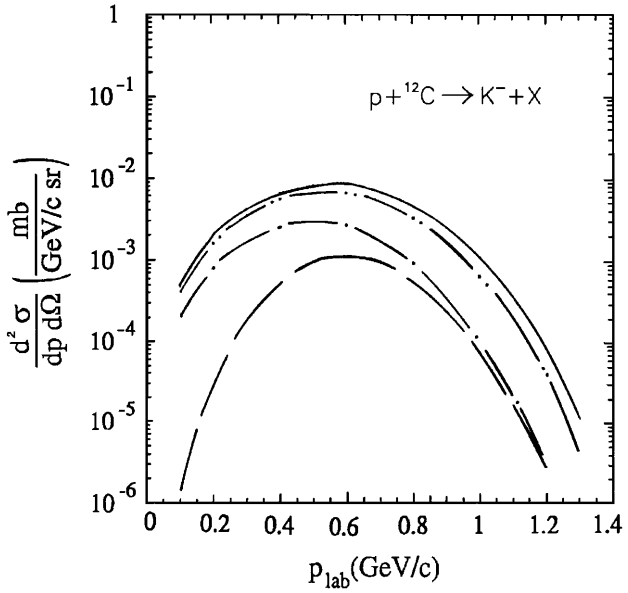

Fig. 7. Double differential cross-sections for the production of K^--mesons at a lab angle of 10° in the interaction of protons of energy 2.3 GeV with ^{12}C nuclei as functions of antikaon momentum. The dashed, dot-dashed, dot-dot-dashed and solid lines are calculations for primary production process (1) with the total nucleon spectral function at $V_0 = 40$ MeV, $U_N^0 = 0$, $U_{K+}^0 = 0$, $U_{K-}^0 = 0$; $V_0 = 40$ MeV, $U_N^0 = 0$, $U_{K+}^0 = 22$ MeV, $U_{K-}^0 = -126$ MeV; $V_0 = 40$ MeV, $U_N^0 = -34$ MeV, $U_{K+}^0 = 22$ MeV, $U_{K-}^0 = -126$ MeV and $V_0 = 40$ MeV, $U_N^0 = -34$ MeV, $U_{K+}^0 = 0$, $U_{K-}^0 = -126$ MeV, respectively.

Thus, our results demonstrate that the measurements of the differential cross-sections for subthreshold "soft" K^- production on different target nuclei will allow to shed light on the antikaon potential in nuclear medium. Such measurements might be conducted at, for example, the accelerator COSY using proton beam in the COSY-ANKE detector system.

4 Summary

In this study we have presented the analysis of the first experimental data [60] on subthreshold K^- production on Be and Cu target nuclei by protons. The measured yields of K^--mesons with momentum of 1.28 GeV/c at a lab angle of 10.5° from p + ^{9}Be and p + ^{63}Cu reactions in the subthreshold energy range were compared with the results of calculations in the framework of an appropriate folding model for incoherent primary proton-nucleon and secondary pion-nucleon production processes, which takes properly into account the struck target nucleon momentum and removal energy distribution, novel elementary cross-section for proton-nucleon reaction channel close to threshold as well as nuclear mean-field potential effects on the one-step and two-step antikaon production processes. It was shown that the effect of the nucleon mean field is of importance in explaining the considered experimental data on "hard" antikaon production, whereas the K^+ and K^- optical potentials play a minor role and the scenario with zeroth K^+ potential is favourable. It was also found that the pion-nucleon production channel does not dominate in the subthreshold "hard" antikaon production in p^{9}Be- and p^{63}Cu-collisions under consideration and the main contributions to the antikaon yields here come from the direct K^- production mechanism, and this offers the possibility to investigate the high-momentum tail of the internal nucleon momentum distribution also *via* the antikaon production on light and medium target nuclei at subthreshold beam energies.

The sensitivity of the subthreshold "soft" antikaon production in p^{9}Be-, p^{12}C-reactions to nucleon, kaon and antikaon effective potentials has been explored. It was demonstrated that, contrary to the case of "hard" antikaon production, the K^- potential has a very strong effect on the K^- yield at subthreshold energies, which is greater than that from nucleon effective potential. This gives an opportunity to determine the antikaon potential experimentally. Therefore, the measurements of the differential cross-sections (spectra and excitation functions) for K^- production on different target nuclei at low antikaon momenta are extremely needed nowadays to achieve a better understanding of the K^- properties in nuclear medium as well as to get a deeper insight into the relative weight of the primary and secondary reaction channels in subthreshold antikaon production and the role played by nucleon-nucleon correlations in this phenomenon.

The author is very grateful to Yu.T. Kiselev and V.A. Sheinkman for their information on experimental results from the ITEP synchrotron on subthreshold antikaon production in proton-nucleus collisions as well as for many valuable and inspiring discussions during the course of this work.

References

1. W. Cassing, E.L. Bratkovskaya, Phys. Rep. **308**, 65 (1999).
2. D.B. Kaplan, A.E. Nelson, Phys. Lett. B **175**, 57 (1986).
3. G.E. Brown, C.H. Lee, M. Rho, V. Thorsson, Nucl. Phys. A **567**, 937 (1994).
4. C.H. Lee, G.E. Brown, D.P. Min, M. Rho, Nucl. Phys. A **585**, 401 (1995).
5. G.E. Brown, M. Rho, Phys. Rep. **269**, 333 (1996); C.H. Lee, Phys. Rep. **275**, 255 (1996).
6. G. Mao, P. Papazoglou, S. Hofmann, S. Schramm, H. Stöcker, W. Greiner, nucl-th/9811021.
7. A. Bhattacharyya, S.K. Ghosh, S.C. Phatak, S. Raha, Phys. Lett. B **401**, 213 (1997).
8. J. Schaffner-Bielich, I.N. Mishustin, J. Bondorf, Nucl. Phys. A **625**, 325 (1997).
9. J. Schaffner, I.N. Mishustin, Phys. Rev. C **53**, 1416 (1996).
10. E. Friedman, A. Gal, J. Mares, A. Cieply, Phys. Rev. C **60**, 024314.
11. M. Lutz, A. Steiner, W. Weise, Nucl. Phys. A **574**, 755 (1994).
12. M.C. Ruivo, C.A. de Sousa, C. Providencia, Nucl. Phys. A **651**, 59 (1999).
13. K. Tsushima, K. Saito, A.W. Thomas, S.V. Wright, Phys. Lett. B **429**, 239 (1998).
14. V. Koch, Phys. Lett. B **337**, 7 (1994).
15. T. Waas, N. Kaiser, W. Weise, Phys. Lett. B **379**, 34 (1996); Phys. Lett. B **365**, 12 (1996).
16. G.Q. Li, C.M. Ko, X.S. Fang, Phys. Lett. B **329**, 149 (1994).
17. E. Friedman, A. Gal, C.J. Batty, Phys. Lett. B **308**, 6 (1993); Nucl. Phys. A **579**, 518 (1994).
18. E. Friedman, Nucl. Phys. A **639**, 511c (1998).
19. T. Kishimoto, nucl-th/9910014.
20. G.Q. Li, C.H. Lee, G.E. Brown, Nucl. Phys. A **625**, 372 (1997).
21. E. Oset, A. Ramos, Nucl. Phys. A **635**, 99 (1998); A. Ramos, E. Oset, nucl-th/9906016.
22. J. Schaffner-Bielich, V. Koch, M. Effenberger, nucl-th/9907095.
23. A. Sibirtsev, W. Cassing, Nucl. Phys. A **641**, 476 (1998).
24. A. Sibirtsev, W. Cassing, nucl-th/9909024.
25. A. Sibirtsev, W. Cassing, nucl-th/9909053.
26. G.Q. Li, C.M. Ko, B.-A. Li, Phys. Rev. Lett. **74**, 235 (1995).
27. G.Q. Li, C.M. Ko, Nucl. Phys. A **594**, 460 (1995).
28. E.L. Bratkovskaya, W. Cassing, U. Mosel, Nucl. Phys. A **622**, 593 (1997).
29. G. Song, B.-A. Li, C.M. Ko, Nucl. Phys. A **646**, 481 (1999).
30. B.-A. Li, C.M. Ko, Phys. Rev. C **54**, 3283 (1996).
31. Z.S. Wang, A. Faessler, C. Fuchs, V.S. Uma Maheswari, D. Kosov, Nucl. Phys. A **628**, 151 (1998).
32. Z.S. Wang, C. Fuchs, A. Faessler, T. Gross-Boelting, Eur. Phys. J. A **5**, 275 (1999).
33. P. Crochet, Nucl. Phys. A **654**, 765c (1999).
34. R. Barth, P. Senger, W. Aher *et al.* (KaoS Collaboration), Phys. Rev. Lett. **78**, 4007 (1997).
35. P. Senger, for the KaoS Collaboration, Acta Phys. Pol. B **27**, 2993 (1996).
36. E. Grosse, Nucl. Phys. A **654**, 501c (1999).
37. F. Laue, C. Sturm, I. Böttcher, M. Debowski, A. Förster, E. Grosse, P. Koczon, B. Kohlmeyer, M. Mang, L. Naumann, H. Oeschler, F. Pühlhofer, E. Schwab, P. Senger, Y. Shin, J. Speer, H. Ströbele, G. Surowka, F. Uhlig, A. Wagner, W. Walus, Phys. Rev. Lett. **82**, 1640 (1999).
38. A. Schröter, E. Berdermann, H. Geissel, A. Gillitzer, J. Homolka, P. Kienle, W. Koenig, B. Povh, F. Schumacher, H. Ströher, Z. Phys. A **350**, 101 (1994).
39. G.Q. Li, C.H. Lee, G.E. Brown, Phys. Rev. Lett. **79**, 5214 (1997).
40. G.E. Brown, C.H. Lee, R. Rapp, Nucl. Phys. A **639**, 455c (1998).
41. G.Q. Li, C.H. Lee, G.E. Brown, Nucl. Phys. A **654**, 523c (1999).
42. W. Cassing, E.L. Bratkovskaya, U. Mosel, S. Teis, A. Sibirtsev, Nucl. Phys. A **614**, 415 (1997).
43. V.P. Koptev, S.M. Mikirtyhyants, M.M. Nesterov, N.A. Tarasov, G.V. Shcherbakov, N.K. Abrosimov, V.A. Volchenkov, A.B. Gridnev, V.A. Yeliseyev, E.M. Ivanov, S.P. Kruglov, Yu.A. Malov, G.A. Ryabov, Zh. Eksp. Teor. Fiz. **94**, 1 (1988).
44. A. Shor, V. Perez-Mendez, K. Ganezer, Nucl. Phys. A **514**, 717 (1990).
45. W. Cassing, G. Batko, U. Mosel, K. Niita, O. Schult, Gy. Wolf, Phys. Lett. B **238**, 25 (1990).
46. A.A. Sibirtsev, M. Büscher, Z. Phys. A **347**, 191 (1994).
47. W. Cassing, T. Demski, L. Jarczyk, B. Kamys, Z. Rudy, O.W.B. Schult, A. Strzalkowski, Z. Phys. A **349**, 77 (1994).
48. A. Sibirtsev, Phys. Lett. B **359**, 29 (1995).
49. H. Müller, K. Sistemich, Z. Phys. A **344**, 197 (1992).
50. M. Debowski, R. Barth, M. Boivin, Y. Le Bornec, M. Cieslak, M.P. Comets, P. Courtat, R. Gacougnolle, E. Grosse, T. Kirchner, J.M. Martin, D. Miskowiec, C. Müntz, E. Schwab, P. Senger, C. Sturm, B. Tatischeff, A. Wagner, W. Walus, N. Willis, R. Wurzinger, J. Yonnet, A. Zghiche, Z. Phys. A **356**, 313 (1996).
51. A. Sibirtsev, W. Cassing, U. Mosel, Z. Phys. A **358**, 357 (1997).
52. S.V. Efremov, E.Ya. Paryev, Eur. Phys. J. A **1**, 99 (1998).
53. E.Ya. Paryev, Eur. Phys. J. A **5**, 307 (1999).
54. A.V. Akindinov, M.M. Chumakov, Yu.T. Kiselev, A.N. Martemyanov, K.R. Mikhailov, S.A. Pozdnyakov, V.A. Sheinkman, Yu.V. Terekhov, *APH N.S.*, *Heavy Ion Physics* **4**, 325 (1996).
55. Yu.T. Kiselev, M.M. Firozabadi, V.I. Ushakov, Preprint ITEP 56-96, Moscow (1996).
56. D. Grzonka, K. Kilian, Nucl. Phys. A **639**, 569c (1998).
57. A. Badala, R. Barbera, M. Bassi, A. Bonasera, M. Gulino, F. Librizzi, A. Mascali, A. Palmeri, G.S. Pappalardo, F. Riggi, A.C. Russo, G. Russo, R. Turrisi, V. Dunin, C. Ekstrom, G. Ericsson, B. Hoistad, J. Johansson, T. Johansson, L. Westerberg, J. Zlomaczhuk, A. Sibirtsev, Phys. Rev. Lett. **80**, 4863 (1998).
58. Yu.T. Kiselev, for the FHS Collaboration: J. Phys. G. **25**, 381 (1999).
59. A.V. Akindinov, M.M. Chumakov, Yu.T. Kiselev, A.N. Martemyanov, K.R. Mikhailov, S.A. Pozdnyakov, Yu.V. Terekhov, V.A. Sheinkman, Preprint ITEP 37-99, Moscow (1999).

60. A.V. Akindinov, M.M. Chumakov, Yu.T. Kiselev, A.N. Martemyanov, K.R. Mikhailov, E.Ya. Paryev, Yu.V. Terekhov, V.A. Sheinkman, Preprint ITEP 41–99, Moscow (1999).
61. S.V. Efremov, E.Ya. Paryev, Z. Phys. A **348**, 217 (1994).
62. X.S. Fang, C.M. Ko., G.Q. Li, Y.M. Zheng, Phys. Rev. C **49**, R608 (1994).
63. G.Q. Li, C.M. Ko, Phys. Rev. C **54**, 1897 (1996).
64. E.L. Bratkovskaya, W. Cassing, L.A. Kondratyuk, A. Sibirtsev, Eur. Phys. J. A **4**, 165 (1999).
65. F. Balestra, DISTO Collaboration, Phys. Lett. B **468**, 7 (1999).
66. E.Ya. Paryev, Preprint INR-1036/2000, Moscow 2000; Yad. Fiz., in the press.
67. P. Moskal, H.H. Adam, A. Budzanowski, *et al.*, nucl-ex/0007018.
68. W. Oelert, Nucl. Phys. A **639**, 13c (1998).
69. C. Gobbi, C.B. Dover, A. Gal, Phys. Rev. C **50**, 1594 (1994).
70. A. Sibirtsev, M. Büscher, H. Müller, Ch. Schneidereit, Z. Phys. A **351**, 333 (1995).
71. E.Ya. Paryev, *Proceedings of the International Conference on Physics with GeV-Particle Beams, 22–25 August 1994, Julich, Germany.* edited by H. Machner, K. Sistemich. (World Scientific, 1995) p. 483.
72. C. Ciofi degli Atti, S. Simula, Phys. Rev. C **53**, 1689 (1996).
73. E.Ya. Paryev, Eur. Phys. J. A **7**, 127 (2000).
74. E. Moeller, L. Anderson, W. Brückner, S. Nagamiya, S. Nissen-Meyer, L. Schroeder, G. Shapiro, H. Steiner, Phys. Rev. C **28**, 1246 (1983).
75. J. Papp, J. Jaros, L. Schroeder, J. Staples, H. Steiner, A. Wagner, J. Wiss, Phys. Rev. Lett. **34**, 601 (1975), Phys. Rev. Lett. **34**, 991 (1975).
76. Yu.T. Kiselev, V.A. Sheinkman, Private communication.
77. S.V. Efremov, E.Ya. Paryev, Z. Phys. A **351**, 447 (1995).
78. A. Sibirtsev, W. Cassing, C.M. Ko, Z. Phys. A **358**, 101 (1997).